REVIEW

A Review on Heavy Metal and Dye Removal *via* Activated Carbon Adsorption Process

SOONMIN HO[1,*,] and MOHAMAD JANI SAAD[2]

[1]Faculty of Health and Life Sciences, INTI International University, 71800, Putra Nilai, Negeri Sembilan, Malaysia
[2]Engineering Research Centre, Malaysian Agricultural Research and Development Institute, 43400, Serdang Selangor, Malaysia

*Corresponding author: Tel: +60 67982000, E-mail: soonmin.ho@newinti.edu.my

Activated carbon could be prepared by using various precursors, which contained carbonaceous materials. In this work, preparation process as well as properties of the obtained activated carbon, removal of heavy metal ions and toxic dyes were reported. The adsorption process was affected under different conditions such as carbonization process, activating agent, adsorbent dose, adsorbate's concentration, agitation process and the pH value. The adsorption data could be observed well fitted with Langmuir, Freundlich, pseudo second order kinetic, pseudo-first order kinetic, Temkin model and other isotherms, if showed the highest correction efficiency value. The spontaneous $(-\Delta G)$, increase in randomness (ΔS), endothermic (ΔH) and exothermic $(-\Delta H)$ could be determined *via* thermodynamic studies.

Keywords: Activated carbon, Adsorption, Carbonization, Activation impregnation, Dye compound, Heavy metal ion.

INTRODUCTION

It is impossible to survive without clean water for any living beings in the earth. The demand for water increased when the world's population continues to grow from time to time [1]. Water pollution will happen when an increasing in the industrial activities. For example, ground water, lake and river get contaminated because of the heavy metal and dyes from the industry [2]. Therefore, several techniques such as adsorption, reverse osmosis, filtration, oxidation, flocculation, magnetic separation, aerobic and anaerobic method could be employed to adsorb these pollutants in wastewater.

Adsorption is a substance or energy attracted to the surface of another material. The attraction between organic matter and activated carbon is an example of adsorption. Organic matter is adsorbed material and adsorbent material is activated carbon. Adsorption is also interpreted as the process of grouping the adsorbed material on the adsorbent surface. The adsorption mechanism between these two materials contains several interactions [3]. Physical adsorption occurs by van der Waals forces (electrostatic forces) such as polarization, bipolar fields and quadratic slope-field interactions, whereas chemical adsorption has a strong interaction between the adsorbent and adsorbate.

It consists of ionic bond or covalent bond [4]. The chemical adsorption energy is higher (40-400 kJ/mol) than the physical adsorption (< 20 kJ/mol) of the physico-chemical adsorption mixture (20-40 kJ/mol) [5]. The differences in the properties of physical adsorption and chemical adsorption [6] can be followed in Table-1.

The propensity of the aqueous solution of the adsorbed material to the adsorbent material is influenced by some factors such as the properties of the aqueous solution of the adsorbent (pH, temperature, ionic strength, competition of organic and inorganic materials), the properties of the adsorbed (structure, functional group, charge density and surface properties) and the properties of the adsorbent (concentration, ion size, ion valence, ion charge, ion weight, stability of the adsorbent and redox standard potential) [7].

Heavy metal waste produced from the manufacturing industries such as industries producing fertilizer, mining, metal plating, batteries contaminate water resources and tanneries [8]. The specific gravity and atomic weight were found to be more than 5 g cm^{-3} and 63.5-200.6 g/mol, respectively [9]. Heavy metals bring high impacts on people, aquatic life (non-biodegradable and stable) and can cause toxicity of human health through food chain [10]. Cadmium and zinc could be

TABLE-1
DIFFERENCES IN THE CHARACTERISTICS OF PHYSICAL ADSORPTION AND CHEMICAL ADSORPTION [Ref. 6]

Physical adsorption	Chemical adsorption
Van der Waals forces, hydrogen bonding and electrostatic forces	Chemical bonding like covalent bonding
Not specific	High specific
Single layer and more	Single layer
Has no relation to adsorbed materials	Has relation to adsorbed materials
Significant at low temperatures	Significant at variable temperatures
Fast, not activated, reversible	Slow, activated and irreversible
There is no electron transfer, although polarization of the adsorbed material occurs	Electron transfer towards bond formation between the adsorbed material and the surface

observed in metal liferous mining and agricultural fertilizers. Nickel and chromium could be seen in electronics and electroplating industries. Lead, mercury and zinc could be found in batteries, paint and pigments industries.

Generally, dye has huge applications including leather, paper, carpet, textile, food and pharmaceutical industrials. Dye contained complex aromatic structure (difficult to degrade), high colour and very high concentration. The production of dye wastewater from modern industries caused seriously environmental pollution. Researchers have highlighted that the dye wastewater treatment process could be identified into three groups (Fig. 1).
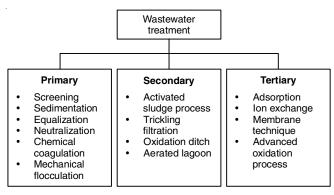

Fig. 1. Dye wastewater treatment by using different techniques

The present work reviews the production of activated carbon by using different precursors. The adsorption capacity of dye and heavy metal ions from wastewater was described. The adsorption kinetic and thermodynamic studies were reported based on different isotherms. The regeneration process was also highlighted.

Activated carbon

Methods of preparation and properties: The activated carbon (AC) is a complex product and its classification is quite complicated based on preparatory methods, unique physical properties, porosity and surface area. However, activated carbon classification is generally directed to its particle size which is classified into as powders, granules and fibers [11]. Activated carbon powders have a particle size of less than 0.1 mm and are generally in the range of 0.015 to 0.025 mm. Its uses are in the treatment of municipal and industrial wastewater, sugar staining, food industry, pharmaceuticals, removal of mercury and dioxins from gas streams [12]. Activated carbon granules range in size from 0.6 to 4 mm. Often used in continuous process applications in the liquid or gas phase. It is better than activated

carbon powder, since it can be reused more than once. Among other advantages include micro pore size distribution, significantly higher density, high hardness properties and low roughness index [13]. Activated carbon fibers (ACF) was produced first in 1970 using rayon raw materials that contain many sources of cellulose and produced by heat treatment in an oxidizing state. Then thermoset polymer materials such as phenolic resins as starting materials in the preparation of ACF. A good raw material must be non-graphical carbon fibers, which are naturally isotropic. The use of cheap starting materials in the synthesis of ACF is still in demand [14].

There are two main processes in the production of activated carbon, namely the carbonation process and the activation process. The carbonization process involves heating the material at a temperature of around 200-800 ℃ in order to dry and evaporate the material in the carbon. During this process, thermal decomposition of the carbon containing material and elimination of non-carbon species have occurred. Stage 1 (starting material was dried) and stage 2 (is known as pre-carbonization phase) are considered as endothermic process, happened when the temperature was less than 200 ℃ and 170-300 ℃. In stage 3 (250-300 C°, exothermic process), generally remove light tar and pyroligneous liquid. Release volatile to enhance the fixed carbon content could be observed in stage 4 when the temperature was more than 300 ℃.

The activation process aims to increase the volume and pores after undergoing the carbonization process and in turn improve the adsorption performance. In general, activated carbon can be synthesized by two methods, namely chemically or physically [15] as indicated in Fig. 2. Physical activation is done by using hot gas or oxidizing gas such as water vapour (steam), air or CO_2 which is flowed on carbonated carbon and burned at 800-1100 ℃. Carbon can be activated by reacting with steam in a closed chamber to enhance gas solid contact [16]. Physical activation is an important step to convert organic matter to primary carbon. The primary carbon contained various types of materials (ash, salt, amorphous and crystalline carbon), undergoes activation/oxidation process at higher temperatures (600-900 ℃) by using carbon dioxide gas or steam.

Chemical activation means that the raw material is mixed with an activating agent (phosphate, carbonate salt, sulfate, chloride, alkali metal hydroxide) or impregnated until a certain time before the activation process is carried out under a rare gas flow [17]. Chemical activation is carried out in which the carbon resulting from the carbonization process is immersed in an activation solution before being activated at a temperature
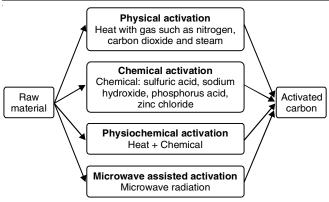
Fig. 2. Different techniques of the activation processes

of 600-900 ºC for 1-2 h. Chemical activation using KOH at a carbon to KOH ratio of 1:4 can achieve the optimal surface area for porous carbon [18]. Under chemical activation process, high specific surface area, formation of OH functional group and good pore development could be observed [19]. There are two types of stages in the chemical activation process, namely single stage activation and two stage activation. One-stage activation means that the carbonization process and activation occur simultaneously while two-stage activation occurs in a separate process, namely the carbonization process is done first followed by the activation process. Two-stage activation is better in activated carbon production than single-stage activation. The carbonization process can remove volatile organic matter and produce porous carbon residue as well as remove tar in the pores. Two-stage activation causes the activating agent to react more with carbon, higher pore volume and surface area [20] could be seen. Carbonization prior to activation helps the formation of early pores to allow the activating agent molecules to easily contact the outer surface of the carbon and form high micro- and meso-pores. It also converts organic matter to a carbon structure and allows the activating agent to perform the activation process.

There are some advantages of activated carbon have been described. For example, higher surface area (up to 3000 m²/g), micro-pores (20-500 Å), excellent adsorption ability and excellent surface reactivity [21]. Activated carbon can adsorb materials in CO_2 gas, urea and others. Activated carbon is also capable of adsorbing dyes, heavy metals, petroleum hydrocarbons, pharma- ceuticals, pesticides and other organics [22]. The use of activated carbon is more widely used in the water treatment, beverages, pharmaceutical industries, automotive and air cleaner

Usage of activated carbon has increased every year. There is 5% increase in activated carbon demand to reach 1.2 million metric tonnes in 2010. For instance, Malaysia has exported activated carbon to Japan (31%), Italy (15%) and the UK (11%). Most activated carbons were made from coconut shells and wood wastes. There are more than 10 companies producing activated carbon in Malaysia with a capacity of 300-1000 tons per month [23]. In 2018, Malaysia exported wood products, wood articles and wood carbon worth US $ 3.58 billion according to United Nations COMTRADE international trade data [24]. The world activated carbon market is worth USD 4.74 billion (in 2015), was expected to achieve USD 8.12 billion (in 2021). In 2015, the market size is 2,743,000 tonnes, was increased to 3,587,000 tonnes (in year 2021).

Activated carbon has two different forms which are in common use, namely the powdered activated carbon (PAC) and granular activated carbon (GAC). In physical, the PAC and GAC were differentiated on their diameter (size of particle). Generally, the re-usage of the activated carbon is commonly on the GAC and not on the PAC due to its small particles to be reactivated. However, few drawbacks also exist while using activated carbon. For examples, growth of bacteria in the filter could be observed (reduce efficiency due to the low contact between the contaminant and adsorbent), therefore, replacement process must be carried from time to time. Also, the dust can cause blockages. The spent carbon was considered as not hazardous, but must be disposed in an appropriate manner.

Adsorption of heavy metal and dyes: The removal of several heavy metal ions (*e.g.* cobalt, mercury, arsenic, copper, lead, chromium, nickel, manganese, iron, aluminium and cadmium) and dye compounds have been discussed by using activated carbon. Table-2 showed the maximum permissible limit of various types of heavy metal ions as highlighted by the Environ-mental Protection Agency (EPA) agency. High surface area, high porosity structure and high adsorption capacity of activated carbon could be produced by using various precursors under specific conditions (carbonation time, carbonation temperature, impregnation ratio, activating agent, *etc*.). The adsorption studies were carried out and investigated *via*

TABLE-2
HEALTH EFFECT AND HIGHEST PERMISSIBLE LIMIT OF DIFFERENT TYPES OF HEAVY
METAL IONS AS SUGGESTED BY THE ENVIRONMENTAL PROTECTION AGENCY (EPA)

Element	Health effect	EPA limit (mg/L)
Cobalt	Asthma; Pneumonia	has not established a reference concentration
Mercury	Allergies; Brain function and DNA damage	0.002
Arsenic	Skin disturbances; Lung irritation	0.01
Copper	Headaches; Liver damage	1.3
Lead	Kidney damage; Disruption of nervous systems	0.015
Chromium	Skin rashes; Lung cancer	0.1
Nickel	Itching; Skin ulceration	has not established a reference concentration
Manganese	Glucose intolerance; Skeleton disorders	0.3
Iron	Lung cancer; Retinitis	has not established a reference concentration
Tin	Liver damage; Depressions	has not established a reference concentration
Aluminium	Dementia; Loss of memory	has not established a reference concentration
Cadmium	Damage to immune system; Bone fracture	0.005

different isotherms. In the following part, the properties of prepared activate carbon, the adsorption capacity and adsorption kinetic of the different adsorbates are briefly discussed based on the literature review.

Cocoa based activated carbon: The cocoa based activated carbon has been produced by using various activating agents. The NaOH impregnated carbon [25] can remove lignin, created accessible surface for adsorption). The adsorption process was considered as endothermic process, spontaneous and obeyed the pseudo-second order kinetic. The highest adsorption capacity of methylene blue was 263.9 mg/g based on the Langmuir model. Ahmad *et al.* [26] reported that adsorption of methylene blue was controlled by film diffusion. Average pore size of 2.7 nm and some functional groups (aliphatic, aromatic hydrocarbon and OH) could be observed in the obtained carbon. Zinc chloride impregnated carbon showed the surface area, pore volume and carbon content were recorded as 780 m^2/g, 0.58 m^3/g and 86.1%, respectively [27]. The percentage of removal of arsenic achieved 80% in less than 60 min in the optimized conditions (pH 6-7, adsorbent dose = 0.5 g/L, initial metal concentration = 100 ppb). Ribas *et al.* [28] reported the highest removal of reactive violet 5 dye was 603.3 mg/g at 298 K in HCl treated carbon. The adsorption process achieved equilibrium after 45 min at pH 2. Mylsamy *et al.* [29] reported the highest adsorption capacity of Reactive Yellow 2 onto the sulfuric acid treated carbon (carbonization temperature and time were 550ºC and 7 h) was 52.63 mg/g according to the Langmuir model (R^2 = 0.997). Adsorption kinetic obeyed pseudo-second order kinetic model (R^2 = 0.99), exhibited the chemisorption process happened (sharing electrons between the activated carbon and dye). Meunier *et al.* [30] revealed that the maximum adsorption capacity (6.2 mg/g) of lead ions could be observed at pH 2, 22 ºC, contact time = 120 min. Recently, León *et al.* [31] prepared cocoa shell-based activated carbon under optimized conditions and evaluated as adsorbent material for methylene blue dye and ferric chloride salt. The activated carbons using dry shell (cocoa shell precursor) were classified into three different particle sizes (8-20, 40-60 and 80-120 mesh), which were obtained by a controlled thermochemical process using a 2^3 factorial experiment design.

Orange based activated carbon: Orange based activated carbon has been synthesized under carbonization process and activation process (activated at 700 ºC for 180 min), exhibited surface area, total pore volume and mean pore diameter were 225.6 m^2/g, 14.5 cm^3/g and 22.4 nm, respectively [32]. SEM images confirmed the significant changes before (homogeneous distribution with cylindrical porous shape) and after (rough surface, covered by dye) the adsorption process. The maximum adsorption capacities of violet B and violet 5R were 38.6-44.2 mg/g and 36.45-37.26 mg/g based on the Langmuir model (R^2 = 0.975-0.996). In the desorption studies, these adsorbents could be used repeatedly for the removal of dye, maintain more than 95% and 90% for violet 5R and violet B, respectively after five adsorption cycles. When the activator was phosphoric acid, the obtained carbon indicated surface area of 1090 m^2/g, mesoporous structure and the acidic character. The results confirmed that the fixed carbon increased, but volatile content

dropped after activation (remove hydrogen and oxygen) and heating process. Adsorption parameters (methylene blue and rhodamine B) followed the pseudo-second order kinetic and Langmuir model. The influence of pH on the adsorption of Direct N Blue 106 onto sulfuric acid treated carbon was studied [33]. In acidic solution, the number positively charged was increased, favoured the adsorption process (highest adsorption of dye was 93.5% at pH 2) because of the electrostatic attraction. While, the hydroxide ions compete with dye anions for the adsorption sites in basic conditions (35.9 to 43.5%). The maximum adsorption capacity of dye was 107.53 mg/g according to Langmuir model (R^2 = 0.976). The adsorption process was heterogeneous process based on the Freundlich model and supported pseudo-second order kinetic isotherm. When the activator was zinc chloride [34], total pore volume and pore diameter were found to be 0.000206 cm^3/g and 20.6Å, respectively. The FTIR studies revealed several functional groups such as OH group (3450 cm^{-1}), CH stretching vibration (2925 cm^{-1}), asymmetric O group (1760 cm^{-1}), symmetric stretching vibration CO (1620 cm^{-1}), stretching vibration COH (1060 cm^{-1}), presented in these carbons. The effect of contact time was studied and observed that removal efficiency increased when the contact time was increased because of prolonged contact between activated carbon surface and the heavy metal ion. The percentage removal was 96% (120 min), 80.2% (210 min), 91.3% (210 min) and 91.2% (240 min) for lead, nickel, chromium and cadmium ions, respectively. Langmuir model studies indicated monolayer adsorption, correlation efficiency values were found to be 0.9059, 0.7947, 0.9377 and 0.9661 in lead, chromium, nickel and cadmium ions, respectively. When sodium hydroxide was activator, it could enhance adsorption capacities. The highest removal of cadmium and nickel was found to be 3 g (91%) and 2.5g (91.11%), respectively [35]. Removal of heavy metal ions increased as the adsorbent was increased, until reached maximum, then no effect due to activated carbon was sufficient to adsorb adsorbate. Thermodynamic studies pointed out that negative value of enthalpy (-39.59 to -53.06 J/mol) and free energy (-284.322 to -431.02 kJ/mol), but positive value of entropy (114.75 o 158.05 J/mol K) during the removal of these ions.

Potato based activated carbon: Potato based activated carbon was prepared by using two activating agents [36]. It was observed that low surface area (4 m^2/g) and pore volume (0.002 cm^3/g) in raw potato peel waste, improved after first activation process (676 m^2/g, 0.26 cm^3/g) due to H$_3$PO$_4$ created new pores, significantly enhanced *via* second activation (KOH) stage, (833 m^2/g, 0.44 cm^3/g) due to removal of specific contents (hydrogen, oxygen and nitrogen) in lignocellulosic biomass. The removal of lead ions was 84.7%, 92% and 97% after 1 h, 24 h and 72 h, respectively. Based on the Langmuir model, the maximum adsorption capacity of cadmium ions was 239.6 mg/g. In the kinetic studies, it was observed that more than 95% of Cd^{2+} ions were adsorbed within 5 min and reached equilibrium within 180 min [37]. Guechi *et al.* [38] prepared activated carbon (mesh size = 0.5 to 2 mm) by using air circulating oven (7 days and 50 ºC) showed the highest adsorption capacity of copper ion was 84.7 mg/g. Removal of acid blue 113 and acid black 1 was observed at pH 2 and pH 3, respectively,

reached equilibrium within 120 min [39]. The highest correlation coefficient (R^2) could be seen in pseudo-second order kinetic and Langmuir model if compared to other models. The adsorption process was endothermic [40], spontaneous, matched well to pseudo-second order and Freundlich isotherm. The highest adsorption capacities of direct red 80 and methylene blue at various temperatures (303.16K to 323.16K) were recorded as 27.778 to 45.45 mg/g and 45.87 to 97.08 mg/g, respectively.

Tomato based activated carbon: Several types of activating agents were used to produce activated carbon. When the zinc chloride was activating agent [41], the physical properties (carbon content = 53.92%, yield = 38.2%, surface area = 1093 m^2/g, total pore volume = 1.569 cm^3/g, average pore diameter = 5.92 nm, meso-porosity = 91.78%) of the obtained activated carbon prepared at the optimized conditions (impregnation ratio was 6:1, carbonization temperature = 600 ºC, carbonization time = 60 min) were reported. Adsorption capacity for metanil yellow dye and methylene blue was 385 mg/g and 400 mg/g, respectively as highlighted in Langmuir model. The highest surface area and micro-pore volume could be observed under the optimized conditions (activation temperature = 700 ºC, impregnation ratio = 2.5, activation time = 60 min) by using $FeCl_2$ activator [42]. $FeCl_2$ could be used to enhance the dehydration process and remove Congo red dye. Mallampati & Valiyaveettil [43] described the fibrous structure (fiber thickness = 9 to 25 µm), with the major constituents (sulphur, oxygen and carbon) based on the scanning electron microscopy (SEM) image and energy dispersive X-ray analysis (EDX) spectrum. Table-3 lists the correlation coefficient (R^2), Langmuir constant (K) and separation factor (R_L) for various pollutants on the adsorbent surface. Regeneration of adsorbent studies revealed that 2% and 96% of pollutants was desorbed at pH 10 and pH 4, respectively indicating H^+ ions replaced cationic pollutants in acidic conditions.

TABLE-3
CHARACTERISTIC OF THE LANGMUIR MODEL
FOR ADSORPTION OF VARIOUS POLLUTANTS
ONTO ADSORBENT [Ref. 43]

Pollutant	K (L/g)	R_L	R^2
Alcian blue	0.0011	0.9947	0.999
Brilliant blue	0.0039	0.996	0.996
Methylene blue	0.0496	0.9527	0.998
Neutral red	00180	0.9822	0.957
Lead ion Pb(II)	0.0081	0.9919	0.994
Nickel ion Ni(II)	0.0001	0.9998	0.997
Arsenic ion As(III)	0.0025	0.9974	0.996
Chromium ion Cr(VI)	0.0044	0.9956	0.992

Avogadro based activated carbon: Avogadro seed consists of 2.78% ash content, 12.67% water, starch, protein, fiber and reducing sugars. Carlos *et al.* [44] demonstrated the synthesis of activated carbon in oven at 375 ºC and confirmed that adsorption is a simple technique to remove mercury ions from wastewater. Chimdessa & Ejeta [45] proposed avocado kernels were impregnated with HCl and K_2CO_3, heated in electric furnace at 800 ºC for 160 min. The activated carbon surface was charged positively (cation was repelled from the adsorbent surface) and

negatively (electrostatic attraction happened) if the pH less than and more than 6.5. The maximum adsorption capacity of copper (16.13 mg/g), lead (7.9 mg/g) and cadmium (142.85 mg/g) were reported based on the Langmuir model (R^2 = 0.998). Haki *et al.* [46] reported different morphologies in the raw materials (flocked texture and irregular shapes) and NaOH treated activated carbon (well development of porosity, increased surface roughness). In the adsorption studies, adsorption of crystal violet dye could be explained through boundary layer diffusion, intraparticle diffusion and adsorption equilibrium stages. Thermodynamic investigations confirmed the spontaneous, decreased in randomness, exothermic process, respectively. In the regeneration studies, this adsorbent showed excellent reusability, the dye desorption was observed to be 76.4% after four adsorption-desorption cycles. Palma *et al.* [47] highlighted the physical properties (surface area = 87.5 m^2/g, mesoporous volume = 74%) of the obtained carbon under optimized carbonation conditions (900 ºC, 65 min). Adsorption of naphthol blue black, reactive black 5 and basic blue 41 onto adsorbent was found to be 10 mg/L, 20 g/L and 13.4 g/L, respectively.

Dragon fruit based activated carbon: The dragon fruit was dried in oven, crushed in to specific size (355 to 850 µm) [48]. The X-ray fluorescence (XRF) showed the percentage of manganese increased from 0.6% to 45.9% after adsorption process. Adsorption data supported Langmuir model (R^2 = 0.9945) with the highest adsorption capacity of manganese was 0.28 mmol/g. The chemisorption occurred based on the pseudo-second order model (R^2 = 0.9997). Sahriani *et al.* [49] stated that the best conditions for removing the copper ions when pH = 4, contact time = 10 min conditions were optimized. The adsorption process fitted well with Langmuir model (R^2 = 0.995) with the highest adsorption capacity was 20.4 mg/g. Tanasal *et al.* [50] demonstrated the maximum adsorption capacity of cadmium ions was 36.5 mg/g according to Langmuir model (R^2 = 0.9913). The best conditions for the removal of cadmium ion were under pH = 5 and contact time was 20 min. Removal of methylene blue dye reached equilibrium after 60 min as reported by Priyantha *et al.* [51]. Based on the Langmuir model (R^2 = 0.972), the maximum adsorption of methylene blue dye was 2 mmol/g. FTIR studies confirmed that some peaks such as 1637 cm^{-1}(C=O), 1244 cm^{-1} (CO *str.*), 1049 cm^{-1} (C-O-C *str.*) were shifted to the new position, indicating these groups were get involved in the adsorption. SEM analysis showed different morphologies before (holes with fibrous-like materials) and after the adsorption of dyes (surface becomes smoother). On the other hand, the mesoporous structure with surface area of 756.3 m^2/g was observed when KOH was employed as chemical activator [52]. The removal of methylene blue dye showed the maximum adsorption capacity was 195.2 mg/g (Langmuir model) could be explained by hydrogen bonding, electrostatic interaction and π-π interaction.

Coconut based activated carbon: Coconut based activated carbon [53] was produced by using carbonization (600 ºC, 180 min, under muffle furnace) and activation process (zinc chloride). SEM images showed smooth surface and rougher morphology in raw material and activated carbon, respectively. Removal of methylene blue dye was fitted well with Langmuir model (R^2

= 0.992, maximum capacity = 324.78 mg/g) than other models [Freundlich (R^2 = 0.89) and Temkin model (R^2 = 0.959)]. The highest percentage of removal of dye reached 92.39% at the optimized conditions (shaking speed = 110 rpm, adsorbent dosage = 0.02 g; initial concentration = 450 mg/L, contact time = 4.5 h). Thermodynamic parameters revealed positive value of enthalpy (7015.76 J/mol) and entropy (26.15 J/mol K), but negative value of free energy (-1559.35 to -2107.78 J/mol). Srisorrachatr *et al.* [54] reported the highest percentage of removal of basic yellow 13 (56.28%) and basic red 14 (55.7%) at pH 11, indicating high electrostatic repulsion at acidic pH conditions. The adsorption data supported the Langmuir model (showed monolayer adsorption) with maximum adsorption capacity of basic red 14 and basic yellow 13 was 22.93 mg/g and 19.76 mg/g, respectively. Bernard & Odigure [55] pointed out the percentage of removal of lead (100%), zinc (26.15%), iron (76%) and copper (71.26%) and reached equilibrium within 40 min, 60 min and 80 min, respectively. In the chemical adsorption process, various types of heavy metals stick to the surface of activated carbon by forming covalent bond. Onyeji & Aboje [56] reported the percentage of removal of Hg^{2+} ions increased from 81-90%, with increasing the adsorbent dose (2 to 12 g), indicating more surfaces were available on the activated carbon. The adsorption data obeyed the Langmuir model (R^2 = 0.96) with the maximum adsorption capacity was 17.24 mg/g. The coconut coir was used to produce carbon by using activating agent (phosphoric acid) [57].

Cucumber based activated carbon: The cucumber peel consisted of cellulose, lignin and hemicellulose components [58]. The removal of lead ions reached equilibrium within 60 min, under optimized conditions (pH = 5 and 30 ℃). The adsorption data supported the Langmuir model (adsorption capacity of lead ions was 133.6 mg/g) and pseudo-second order kinetic model. Removal of cadmium by using activated carbon has been reported by Mousumi *et al.* [59]. FTIR studies confirmed the carboxyl group was considered as metal-binding group during the adsorption process. The adsorption data supported Langmuir model (maximum adsorption capacity of cadmium = 0.998 mmol/g) and pseudo-second order kinetic isotherm. The sulfuric acid treated activated carbon [60] showed unique properties (moisture = 11.62%, ash = 12.59%, zero-point charge = pH 4, conductivity = 0.922 μs cm⁻¹ and total acidic group = 0.192). When the pH was increased, more negative charged could be observed in the adsorbent surface, strong electrostatic attraction appeared between dyes and activated carbon (maximum adsorption occurred). The maximum adsorption capacity of crystal violet and rhodamine B dyes was 35.33 mg/g and 34.01 mg/g, respectively based on the Langmuir model. The chemisorption process and intraparticle diffusion was not the only rate controlling step as highlighted during the experiment. The influence of agitation speed was studied by Vasu & Selvaraju [61]. The percentage removal of reactive blue dye increased from 94.4, 94.6, 94.7 and 94.9% with increasing the speed from 50, 100, 150 and 200 rpm. The maximum adsorption capacity of dye reached 59.17 mg/g based on the Langmuir model (R^2 = 0.9891). The adsorption kinetic obeyed pseudo first order model (R^2 = 0.9915) with rate constant and equilibrium

adsorption intensity were 0.0694 min⁻¹ and 133.23 mg/g, respectively.

Papaya based activated carbon: Activated carbon can be prepared by using different parts of papaya. Adsorbent produced by using papaya seed showed big pore size with mesoporous texture [62]. The adsorption data could be represented by pseudo-second order model and Langmuir isotherm (highest adsorption capacity of direct black 38 = 440 mg/g). The adsorption process was successfully controlled by pore diffusion and external mass transfer. The papaya leaf was used as staring material as reported by Ahmaruzzaman [63]. The highest removal of methyl orange dye could be found in the specific conditions (pH = 2, contact time = 2 h, agitation rate = 150 rpm). The adsorption kinetic supported pseudo-second order model and Langmuir model (highest adsorption capacity = 333.34 mg/g). Igwegbe *et al.* [64] reported the best adsorption process happened at pH 5.9 with 5 g/100 mL adsorbent, 0.8 g (zinc), 0.042 g (cadmium) and 0.047 g (lead) were successfully removed onto papaya trunk based activated carbon. Saeed *et al.* [65] employed papaya wood as precursor to remove copper ions in wastewater. The highest removal of copper ion was 97.8% in the specific conditions (concentration of copper = 10 mg/L and adsorbent dose = 5 g/L, pH = 5). The adsorption data supported Langmuir model (R^2 = 0.99) and pseudo-second order kinetic isotherm (R^2 = 0.99). It was noted that no loss in the efficiency of Cu^{2+} ions removal (after five adsorption cycles) in biosorption-desorption investigations.

Cotton based activated carbon: The cotton fiber, stem and stalk have been used to produced activated carbon. The characteristics of cotton stem based activated carbon [66] were reported such as moisture (7%), ash (24%), density (0.431 g/cc) and surface area (198 m²/g). The adsorption of Sudan Red G dye increased when the contact time was increased, then reached equilibrium (maximum adsorption = 91.27%) after 2 h. It was clear that percentage of removal increased (90.54% = maximum adsorption) as adsorbent dose (0.002 to 0.01 g/L) was increased because of the large surface area and more functional groups on the surface of adsorbent. Based on the Langmuir model (R^2 = 0.877), maximum adsorption capacity was 25 mg/g. The activated carbon was produced from cotton stalk [67], had surface area about 850 m²/g with the particle size (35-50 mesh fraction). The pH of zero point of charge was 5.6, indicating adsorbent has negative charge when the pH more than pH 5.5. The experimental findings confirmed that the removal of lead (99% when pH < 5), copper (99%, pH < 6.3) and cadmium (80% for pH 9) strongly depended on the pH conditions. High quality of carbonaceous material could be prepared under carbonization process by using acid or base treatment process (to remove lignin and hemicellulose components) [68]. The cellulose rich materials showed the fastest removal of methylene blue dye onto cotton stalk based carbon within the test time. Cellulose can produce fibrous network structure (due to intermolecular hydrogen bonding), can enhance pore size and pore volume. It was observed that the adsorption process was physio-sorption and high concentration of methylene blue dye needed longer time to achieve equilibrium process. Concentrated sulfuric acid was used as activating agents to

synthesis cotton fiber based carbon to remove azo dyes [69]. The results revealed that adsorption of dye rapidly in first 20 min (dye ion was adsorbed by exterior adsorbent surface), adsorption rate dropped and achieved equilibrium about 1 h (completely adsorbed by interior adsorbent surface).

Rice husk based activated carbon: The synthesis of rice husk based activated carbon by using different activating agents. The char could develop more pores after activation process by using zinc chloride. The highest removal capacity of crystal violet was 61.575 mg/g [70] and the adsorption data obeyed pseudo second order model and intra particle diffusion model. Ahiduzzaman & Sadrul Islam [71] reported that the obtained activated carbon consisted of high amount of silica. Development of porosity could be achieved by removing silica through higher temperature. The uptake of methylene blue dye was observed to be 149, 203, 262 and 264 mg/g when the temperature was increased (600, 700, 800 and 900 ℃). The highest correlation coefficiency could be seen in Langmuir model (R^2 = 0.94) and pseudo-second order model (R^2 = 0.998). The adsorbent was treated with sulphuric acid as reported by Emadi & Zare [72]. The highest removal of basic fuchsin dye achieved when use 100 mg of dye/1g of adsorbent and obeyed the Langmuir model. The physical properties [yield = 49.3%, moisture (4.86%), ash (30.04%) and volatile matter (15.7%) of HCl treated carbon (size = 100 meshes] were studied [73]. The maximum adsorption capacity of lead was 0.567 mg/g in car battery wastewater under specific conditions (carbonization time = 150 min, carbonization temperature = 500 ℃). The rice hull based activated carbon was produced *via* carbonization (in muffle furnace, 400 ℃, 60 min) and activation (NaOH, 70 ℃, 24 h) process [74]. The results showed that removal of aluminium and iron ions was increased, reached maximum after 3 h. The highest adsorption capacity of aluminium and iron ion was observed to be 34.48 mg/g and 45.45 mg/g, respectively as indicated in Langmuir model (R^2 = 0.98). The adsorption free energy was found to be 8-13 kJ/mol in both metal ions as highlighted in the Dubinin-Radushkevich model, indicating the chemisorption process. Generally, the physical and chemical adsorption took place when the adsorption free energy was less than 8 kJ/mol and 8-16 kJ/mol.

Hazelnut based activated carbon: The hazelnut based activated carbon was produced *via* carbonization (500 ℃ for 2 h) and activation (phosphoric acid) process [75]. Based on the Langmuir model (R^2 = 0.963-0.9914), maximum adsorption capacity of reactive red 2 dye increased (12.2 mg/g to 136.98 mg/g) when the temperature was increased from 283 K to 318 K. The obtained zinc chloride treated carbon showed the surface area about 1092 m²/g [76]. The maximum adsorption capacity of copper and lead was 6.645 and 13.05 mg/g, respectively according to Langmuir model. Other heavy metal ions such as aluminum (7.75 mg/g), chromium (7.36 mg/g), iron (5.47 mg/g), arsenic (7.39 mg/g) and cadmium (4.55 mg/g) fitted well with the Langmuir model [77]. The influence of pH on the adsorption behaviour was studied by Veselin *et al.* [78] Lower adsorption of methylene blue in the acidic conditions due to the neutralization of hydroxyl group (from surface of adsorbent) with H^+ ion (from HCl solution during pH adjustment). The

highest percentage of removal of dye reached 97% at pH = 5.3.

Coffee based activated carbon: The physical properties of the activated carbon strongly depended on the preparation conditions. The coffee residues were dried in convection oven, 24 h at 60 ℃ [79] and indicated unique characteristics (surface area = 187 m²/g, total pore volume = 8.94 m³/g and average pore diameter = 24 nm). The highest correlation coefficiency value in Langmuir model (R^2 = 0.9887), with the maximum adsorption capacity of methylene blue was 4.68 mg/g. Nakamura *et al.* [80] reported the surface area (0.17 to 61.71 m²/g) and pore volume (0.001 to 0.041 mL/g) increased when the carbonization temperature was increased from 800 to 1200 ℃. It was concluded that the adsorption of acid orange 7 was controlled by intraparticle diffusion process. The equilibrium amount of dye (acid orange 7) adsorbed onto adsorbent was found to be 1.01 mg/L, 3.12 mg/L, 6.02 and 3.09 mg/L, 13.38 mg/L, 14.51 mg/L, when the concentration of dye was 100 and 500 mg/L, respectively, the carbonization temperature increased from 800 to 1200 ℃. Block *et al.* [81] described that higher carbon content (70.3% to 82.4%) could be observed after pyrolysis process if compared to raw material (56.9%). In thermogravimetric analysis, the evaporation of water occurred at 100 ℃, decomposition of cellulose, hemicellulose and lignin happened at 200-450 ℃ and decomposition of the carbon at 1000 ℃. The results confirmed that non-pyrolyzed raw material adsorbed nearly no methyl orange dye, while material pyrolyzed only removed below 20% of dye. On the other hand, higher metal removal (copper and chromium ions) was observed in treated coffee residue based carbon. The kinetic constant values for the removal of copper ion were found to be 0.032 and 0.037 min⁻¹ in untreated and treated activated carbon, respective based on the pseudo-first order isotherm (R^2 = 0.995-0.998) [82]. The maximum adsorption capacity of chromium ions was 38.68 mg/g and 43.75 mg/g in untreated and treated activated carbon, respectively based on the Langmuir model (R^2 = 0.995). The influence of agitation rate was studied and the optimum speed should be 140 rpm. In case of chromium and copper ions, it is difficult to find active sites at low speed (60-80 rpm). High portions of mesoporous structure could be produced by using zinc chloride and KOH, carbonized in nitrogen atmosphere and activated with carbon dioxide conditions [83]. Maximum porosity could be seen when the impregnation ratio was increased due to release of tars from crosslinked framework. The highest surface area could be observed because of the potassium intercalated to carbon matrix, widened the space between carbon atomic layers. Removal of mercury ions reached 0.002 to 0.38 mmol/g, the carbon (surface area = 1058 m²/g, mesoporous volume = 0.34 cm³/g and total pore volume = 1.23 cm³/g).

Palm shell based activated carbon: The palm shell was crushed (powder size = 710 μm) then dried for 240 min at 110 ℃ [84]. Removal of rhodamine 6G achieved equilibrium in 2 h, could be considered as chemisorption process (pseudo-second order model). The maximum adsorption capacity reached 19.65 mg/g based on the Langmuir model (R^2 = 0.981). Negative value in free energy represented adsorption was spontaneous in nature. The surface area and micro porosity structure were

observed to be 1058 m²/g and 721 m²/g, respectively when the activating agent was zinc chloride [85] and under specific carbonization conditions (550 °C for 60 min). The highest uptake of methylene blue dye was 225.3 mg/g in specific conditions (raw material: $ZnCl_2$ ratio was 1:1, carbonization temperature = 550 ºC). Mook *et al.* [86] highlighted the removal of reactive black 5 dye was favourable by using Freundlich model (R^2 = 0.996) when the pH was 2, however, obeyed Langmuir model at higher pH such as pH 6 (q_m = 23.6 mg/g) and pH 10 (q_m = 24.86 mg/g). The adsorption process was endothermic with low activation energy (12.6 kJ/mol) and the adsorption kinetic followed pseudo-first order model. On the other hand, removal of various types of heavy metals reached equilibrium within 2 h [87]. The percentage of removal and the rate constant values (pseudo-second order) of Cr^{6+}, Pb^{2+}, Cd^{2+} and Zn^{2+} ions were 98.92%, 99.01%, 84.23%, 83.45% and 1.2×10^{-5}, 3×10^{-5}, 1.2×10^{-5}, 2.4×10^{-5} mg/min, respectively. Shaukat *et al.* [88] reported that the moisture content, volatile content and ash content were reduced after carbonization process (rotary kiln, 10 min, 800 ºC). The HCl-NaOH treated activated carbon showed the lowest ash (4.5%), moisture content (6.5%), but the highest surface area (149.6 m²/g) indicating strong adsorbent properties and well developed porosity. Removal of nickel and copper ions followed Freundlich model and pseudo-second order isotherm, respectively. The highest removal of copper and nickel was observed to be 97.3% (120 min) and 96.7% 210 min), respectively. The crushed palm kernel shells were carbonized in the cylindrical vertical furnace (700 ºC for 2 h, nitrogen gas flow rate = 0.5 L/min), impregnated with KOH (impregnation ratio = 4:1) as reported by Saber *et al.* [89].

Walnut based activated carbon: Synthesis of activated carbon through chemical activation process (zinc chloride) was done at 900 ºC. The X-ray diffraction (XRD) studies revealed the amorphous phase and crystalline phase due to the lignin and cellulose, respectively. The Q_{sat} increased from 281.45 mg/g to 442.556 mg/g when the temperature was increased from 298 K to 318 K. The measurement of adsorption energies revealed that during the endothermic process, the physical interaction was accounted for the removal of Congo red. The zeta potential was -13.47 mV when the pH was 7 indicating the presence of acidic groups in adsorbent [90]. The powdered form (200-350 µm) of NaOH treated activated carbon was prepared and showed unique characteristics (surface area = 2.505 m²/g, average pore diameter = 13.094 nm, pore volume = 0.0082 cm³/g) [91]. Based on the SEM analysis, a hollow, high porosity and hard surface could be observed before the adsorption, however, accumulated the spherical shape could be found after methylene blue dye adsorbed on the surface of adsorbent. The removal of methylene blue dye increased when the agitation speed was increased until 200 rpm due to kinetic energy of the activated carbon and methylene blue dye was increased. Motahare *et al.* [92] used the same activating agent as well. These NaOH-treated carbons showed surface area, total pore volume, mean pore diameter and micropore volume of 2.095 m²/g, 0.0171 cm³/g, 32.64 nm and 0.48 cm³/g, respectively. The opitimum conditions were pH = 7, contact time = 13 min, room temperature, adsorbent dose = 0.8 g/L. Based on the Langmuir model, maximum

adsorption capacity was 146.4 mg/g and 123.2 mg/g for brilliant green and crystal violet, respectively.

Tarap based activated carbon: Tarap based activated carbon (355 µm = diameter) was prepared by Dahri *et al.* [93]. According to the kinetic parameters, the chemisorption and electrostatic interaction could play important role in the adsorption. The point of zero charge was found to be 4.20, indicating that at lower pH value, more positive charge could be observed in the surface of adsorbent because of the protonation of the functional groups. The positive value in enthalpy (5.1 kJ/mol) and entropy (30.5 J/mol K) represented endothermic and increased in randomness in the adsorption process. However, the negative value in free energy (-4 to -5.2 kJ/mol) represented adsorption process became more favourable at higher temperature (298 K to 343 K). Langmuir model showed the highest R^2 value (R^2 = 0.987) with maximum adsorption capacity of crystal violet (q_m = 217.03 mg/g) if compared to Freundlich model (R^2 = 0.981) and Tempkin model (R^2 = 0.952). In the regeneration study, this adsorbent maintains adsorption of dyes even after five adsorption cycles.

Sago based activated carbon: Sago waste based activated carbon was prepared through the chemical activation (sulphuric acid and ammonium persulfate), grounded and sieved (125-250 µm). Physical properties such as yield (78%), ash (12%), density (0.75 g/mL), pore volume (0.67 mL/g), porosity (80%) and BET surface area (625 m²/g) were reported. Several groups (carboxyl, carbonyl, phenolic and lactonic) could be observed in the obtained carbons. It was observed that copper(II) ions adsorption [94] was 15.3, 20.08, 25.78 and 30.79 mg/g when the concentration was found to be 20,30, 40 and 50 mg/L, respectively at equilibrium time. The equilibrium parameter was observed less than 1 (0.043 to 0.31), indicating the favourable adsorption process based on the Langmuir model. On the other hand, the SEM and FTIR spectra showed the cave opening on the surface of the adsorbent and the presence of starch and cellulose moieties in the sample [95]. Removal of Alizarine red S dye increased when the agitation speed was increased (from 50 to 250 rpm) due to reduce in boundary layer thickness around the activated carbon. The adsorption process was favourable as indicated in Langmuir model (R^2 = 0.98). The negative value of free energy (-8.2159), enthalpy (-8.15) and entropy (-0.0554) represented the spontaneous, exothermic and reduced in randomness at the solid/solution interface. Zainab *et al.* [96] proposed that preparation of activated carbon *via* microwave pyrolysis and chemical activation process (NaOH) showed the unique properties (surface area = 471.1 m²/g, average pore size = 36.29 µm). Removal of lead (89.8%), chromium (47%) and zinc (18.4%) was reported under optimized experimental conditions (adsorbent dose = 1 g/50 mL, contact time = 24 h, mixing speed = 150 rpm, initial concentration = 5 mg/L).

Rubber based activated carbon: The rubber leave and rubber seed could be used to produce activated carbon. Mono-layer adsorption capacity of basic blue 3 was observed to be 227.27 mg/g, at 30 ºC onto rubber seed coat based activated carbon [97]. The adsorption data supported Freundlich model and pseudo-second order kinetic model. Linh *et al.* [98] reported that higher temperature (< 60 ºC), small particle size such as

45-63 μm (due to free from the mass transfer effect) and high pH value (< pH 5) were required to remove malachite green dye from aqueous solution. The adsorption data fitted well with Langmuir isotherm ($R^2 = 0.99$) with the maximum adsorption capacity of 27.4 mg/g. Removal of various concentrations of lead ions on to rubber leave based activated carbon [99] was well-esblished. The experimental results confirmed 20 mg/L lead solution reached equilibrium easily due to sufficient adsorption sites if compared to 50 mg/L. The adsorption data obeyed pseudo-second order kinetic ($R^2 = 0.998$) and Freundlich model ($R^2 = 0.996$). The negative value of entropy (112.18 J/mol K), free energy (-4.41 to -6.63 kJ/mol) and enthalpy (-40.44 kJ/mol) could be observed based on the thermodynamic studies.

Rambutan based activated carbon: Rambutan based activated carbon has been prepared under the specific conditions. Malachite green dye adsorption uptake was observed to be increased when the contact time, initial concentration and solution temperature were increased [100]. The highest correlation coefficiency was observed in the pseudo-second order kinetic model and Freundlich model. The optimization studies on the adsorption of malachite green were carried out by Syahidah *et al.* [101]. Percentage of yield was 22.56% and removal of dye reached 91.45% under specific conditions (activation temperature = 802 ℃, activation time = 60 min, impregnation ratio of KOH:charcoal = 2.4). Thermodynamic studies revealed negative value of free energy (spontaneous process) and positive value of enthalpy (endothermic process). Adsorption kinetic data supported pseudo-second order model and the mechanism of adsorption was controlled by intraparticle diffusion. Rambutan peel was used to synthesize activated carbon under KOH and carbon dioxide (CO_2) gasification [102]. The best experimental conditions (activation temperature = 789 ℃, activation time = 1.8 h, impregnation ratio = 3.5) results in the percentage of removal of 18% and 78.38% of remazol brilliant blue R reactive dyes. Similarly, Tarigan *et al.* [103] used Rambutan rod based carbon for the remove copper ions. Based on AAS analysis, 43456 ppm of copper was adsorbed within 120 min. Rinadi *et al.* [104] reported that delignification is an important step to remove heavy metal ion effectively. FTIR and SEM analysis showed the loss of lignin (disappeared peaks at 1716.81 and 1216.6 cm^{-1}) and more porous in the adsorbent, respectively. Adsorption capacity was 64.015 mg/g for nickel(II) ion and obeyed Freundlich model.

Cempedak based activated carbon: Cempedak based activated carbon could be used to remove acid blue 25, methylene blue and brilliant green dyes effectively. The preparation of activated carbon through chemical activation (phosphoric acid), under heating process [105]. When the activated carbons were calcined at 450 ℃, water content was 7.1% and the adsorption capacity of methylene blue dye was 98.88%. The XRD data confirmed the obtained carbons were amorphous structure. The experiments were carried out and showed maximum adsorption capacity of brilliant green was 0.203 mmol/g based on the Langmuir model [106]. FTIR spectra revealed some functional groups such as OH, C=C, C=O an H-N get involved during the adsorption process. The adsorption was endothermic (enthalpy = 12 kJ) and obeyed the pseudo-second order kinetic

order. Khairud *et al.* [107] reported the adsorption of acid blue 25 dye was endothermic, showed the maximum adsorption capacity of 6.6 mg/g as indicated in the Langmuir model. Regeneration investigation confirmed this adsorbent could maintain its adsorption capacity even after five adsorption cycles.

Mango based activated carbon: The mango pod, leave and peel can be used to synthesize activated carbons. The adsorption capacity of Cr(III) ions and iron(II) ions was 237.5 mg/g and 227.5 mg/g under the specific conditions (mango leave based activated carbon dose = 100 mg/L, concentration of adsorbate = 50 mg/L) [108]. The adsorption data followed the Freundlich model ($R^2 = 0.928$-0.976) and pseudo-second order kinetic model ($R^2 = 0.999$). Based on the thermodynamic studies, the enthalpy, free energy and entropy value were found to be 22.86-34.68 kJ/mol, -8.62 -13.32 J/mol K and 142.25 -3108.33 kJ/mol, respectively. The orthophosphoric acid modified mango pod was used to remove rhodamine B dye. During the experiment, there are different techniques, namely the experimental data (456.67 mg/g), artificial neural network (389.5 mg/g) and adaptive neuro fuzzy inference systems (410.56 mg/g) were used to study the adsorption capacity of dyes [109]. The mango peel based activated carbon was synthesized in the presence of nickel to improve regenerability and efficiency of the adsorbent [110]. The obtained adsorbent successfully removes rhodamine B (98%) and manganese ions (93%). According to regeneration investigation, adsorption efficiency was 88.7% and 85.2% for rhodamine B and Mn^{2+}, respectively after the 5th adsorption cycles. The Langmuir model and pseudo-second order model can be employed to demonstrate the favourable adsorption of these adsorbates.

Mangosteen based activated carbon: The field emission scanning electron microscopy (FESEM) and FTIR analysis demonstrated that methylene blue dye can be adsorbed onto the mangosteen based activated carbon due to the electrostatic interaction between cationic (methylene blue) and specific surface function group of the adsorbent [111]. Removal of dye achieved 99.7% under specific conditions (adsorbent dose = 5 g/L, particle size = less than 75 μm, contact time = 10 min). Ahmad & Alrozi [112] reported the synthesis of activated carbon under KOH, through CO_2 gasification process. The obtained absorbent showed percentage of yield was 20.76% and removal of remazol brilliant blue R dye (80.35%) under the optimized experimental parameters (activation temperature = 828 ℃, activation time = 60 min, KOH impregnation ratio = 3). On the other hand, the physical properties of obtained K_2CO_3 treated activated carbon (average pore diameter = 1.82-2.71 nm, micropore volume = 0.32-0.34 cm^3/g, micropore area = 659-702 m^2/g, total pore volume = 0.43-0.75 cm^3/g, specific surface area = 908-1106 m^2/g and yield = 20.3-23.1%), based on the Langmuir model, the highest adsorption capacity (q_{max}) of copper ions was found to be 21.74 mg/g. Moreover, regeneration efficiency was found about 93.1% and 83.4% for 2nd and 3rd adsorption cycles, respectively [113].

Apricot stone based activated carbon: Production of activated carbon through chemical activating gent (phosphoric acid) under 500 ℃, 120 min in muffle furnace [114]. The highest removal of aluminium and zinc were 92.86% (pH 6)

and 93.88% (pH = 6.5), respectively at specific pH value. Based on the thermodynamic parameter analysis, positive value of entropy (95.6 to 182.9 J/mol K), positive value of enthalpy (24.1 to 50.698 kJ/mol) and negative value of free energy (-4.279 to -7.16 kJ/mol) could be found, representing increasing randomness, endothermic and spontaneous process. Abbas [115] concluded that the highest removal of lead and cobalt were 80.6 mg/g (pH 8) and 25.22 mg/g (pH 9), respectively under different pH values. The adsorption was exothermic process, fitted well with Langmuir model and pseudo-second order model.

Sugarcane based activated carbon: Removal of lead, nickel, iron, zinc and methylene blue dye strongly depended on the optimum experimental conditions. The nitrogen adsorption desorption isotherm has been investigated and showed type II (sigmodal shape). Other physical properties (pore diameter = 57.285 Å, specific surface area = 0.734 m^2/g and pore volume = 0.000679 cm^3/g) were reported [116]. The zero-point charge was 4.69, indicating positively charged on the surface of adsorbent when the pH was below 4.69. The highest adsorption capacity of methylene blue dye reached 49.26 mg/g based on the Langmuir model and the adsorption kinetic obeyed the pseudo-second order kinetic model (R^2 = 0.997 to 1). The thermodynamic parameters indicated the exothermic process (enthalpy = -31.062 kJ/mol), spontaneous (free energy = -1.83 to -6.8 kJ/mol) and reduced in molecular disorder (entropy = -0.084 kJ/mol K). Phosphoric acid was used during the chemical activation process [117]. Adsorption of heavy metal ions increased with the contact time, then became stable. Because of many active sites are available at the beginning of time, following that these sites successfully connected to the heavy metal ions after certain times. The highest percentage removal of Fe and Zn was observed to be 78% and 85% within 120 min. Ezeonuegbu *et al.* [118] reported the removal of nickel(II) ions (96.33%) was higher if compared to lead(II) ions (8.3%) due to Ni(II) ions showed higher affinity towards the activated carbon.

Bamboo based activated carbon: Bamboo has also been employed in the construction sites and living facilities due to very tough, strong and cheap materials. Various types of activating agents such as phosphoric acid, humic acid and trioxonitrate(V) acid were used to prepare activated carbon. The fixed carbon content increased (11.32%, 73.15% and 76.86%), however volatile matter decreased (70.12%, 16.21% and 10.64%) in bamboo, bamboo charcoal and bamboo activated carbon respectively. Low ash content is required to synthesize the most active product. The presence of ash (calcium, iron, silica, alumina, magnesium) will disturb the adsorption process due to competitive adsorption and catalysis of adverse processes. At higher temperature (carbonization and activation), the fixed carbon content has been significantly changed due to volatile content was decomposed. Santana *et al.* [119] reported that the synthesis of activated carbon (surface area = 1354.42 m^2/g) by using phosphoric acid following that with the water steam (500 ºC, 60 min). The adsorption process reached equilibrium after 12 h. The maximum adsorption capacity of methylene blue dye was 374.75 mg/g based on the Langmuir model (R^2 = 0.968). Removal of chromium ions onto bamboo bark based carbon by using humic acid was reported by Zhang *et al.* [120].

Removal of Cr(VI) ions matched well with Freundlich model (R^2 > 0.99) and pseudo-second order kinetic model (R^2 > 0.99). The results confirmed the best removal of chromium ions when the concentration of humic acid and the pH value were 10-20 mg/L and pH 2 to 9, respectively. Chan *et al.* [121] confirmed the removal of acid dyes followed Freundlich and Langmuir models. The experimental results indicated that the smaller size (acid blue 25 dye) could be adsorbed easily onto the surface of activated carbon if compared to bigger size (acid yellow 117 dye). Ademiluyi & Ujile [122] used trioxonitrate(V) acid as activating agent to prepare activated carbon, which exhibited the bulk density and ash content of 0.458 g/mL and 2.76%, respectively. It was observed that the highest removal of iron ion could be observed within 30 min with reduction of particle size (> 150 µm). The highest adsorption capacity of iron(III) ion achieved 166.7 mg/g according to Langmuir model (R^2 = 0.994). Bamboo stem [123] was used to synthesize activated carbon by using phosphorus acid (activating agent). The fixed carbon, volatile content and moisture content were 62.45%, 24.4% and 7.6%, respectively. The experimental findings confirmed that the equilibrium adsorption was achieved at 1 h when the concentration of lead ion was 30 mg/L (96.07%) and 2 h for 60 mg/L (90.2%) and 90 mg/L (85.16%). Removal of lead(II) ion was favourable and obeyed the Freundlich model (R^2 = 0.935).

***Moringa oleifera* based activated carbon:** Several parts such as pods, leave, seed, wood, bark and husks were used to prepare the activated carbon at specific conditions. McConnachie *et al.* [124] proposed that the best conditions for preparation of activated carbon from pods and husks (surface area = 713 m^2/g) were 650 ºC, 30 min and 800 ºC, 30 min, respectively. Removal of methylene blue reached equilibrium within 90 min, could be classified as physical adsorption and exothermic process [125] when the leave was used as starting material (under NaOH activation). The best experimental conditions were pH = 7 and adsorbent dosage = 1.67 g/L. Reck *et al.* [126] reported the removal of tartrazine (yellow dyes) from moringa seeds (raw material). Removal of dye reached 95%, achieved the highest capacity of 91.27 mg/g, when the temperature was 15 ºC. The adsorption process was endothermic, matched well with the Freundlich model, pseudo-first order model. Matouq *et al.* [127] studied the adsorption of various types of heavy metal ions *e.g.* nickel (Temkin, Dubinin-Radushkevich), copper (Freundlich, Temkin model) and chromium (Langmuir model) from wastewater by using different isotherms. The adsorption capacity was found to be 6.07 mg/g, 5.53 mg/g and 5.497 mg/g for copper, nickel and chromium, respectively by using moringa pods. The surface area (439.23 m^2/g) and pore volume (0.189 cm^3/g) were investigated [128] in bark based activated carbon (activation agent = zinc chloride and sulfuric acid, 700 ºC for 1 h). The pores have been successfully filled-up by heavy metal ions after completed adsorption process as indicated by the FESEM analysis. The experimental findings confirmed the highest removal capacities of copper and cadmium ions, estimated to be 20.43 mg/g and 17.01 mg/g, respectively as stated in Langmuir model. The adsorption kinetic data perfectly matched with pseudo-second order model (R^2 = 1 for copper, R^2 = for cadmium). Zawani *et al.* [129] reported the synthesis of activated

carbon from moringa wood, impregnated with phosphoric acid, at 673 K for 60 min. The maximum removal of nickel(II) ions (8.043 mg/g) in the specific conditions such as adsorbent dosage = 0.1 g, contact time = 120 min, concentration of iron = 10 mg/L.

Maize cob based activated carbon: The maize cob based activated carbon can be used to adsorb acrylic blue G, safranin basic dye, methylene blue and lead(II) ions. The maize cob has been used to produce activated carbon in the presence of phosphoric acid, under 500 °C for 2 h [130]. The best conditions for the removal of acrylic blue-5G dye such as pH of dye = 8 to 10, adsorbent dosage = 0.1 g, stirring rate = 20 rpm. The corncob based activated carbons were prepared under various activation temperatures [131]. Surface area (700 to 600 m²/g) and micro pore volume (0.011 to 0.003 cm³/g) decreased with increasing the temperature from 400 to 600 °C. While, the point of zero charge and the iodine number values were found in the range of 5.7-7.4 and 485-945 mg/g, respectively. Adsorption of methylene blue obeyed the Langmuir model when at 400 °C (q_m = 28.65 mg/g) and 500 °C (q_m = 17.57 mg/g). Choi & Yu [132] reported that the methylene blue dye could be removed by using 10 g/L of activated carbon, if the concentration less than 0.005 g/L. Also, the highest adsorption capacity reached 417.1 mg/g based on the experimental results. While, Preethi *et al.* [133] also utilized maize cob based activated carbon for the removal of safranin basic dye by increasing the temperature, varying adsorbent dosage and smaller mesh size. The adsorption kinetic data supported the first order reaction, Langmuir and Freundlich models. The results revealed the best adsorption when the pH was in the range from pH 5 to pH 9. Thermodynamic studies showed endothermic process and the enthalpy value was 35.6 kJ/mol. Characteristic of the obtained carbons including moisture content, pH, density, particle size and surface area were observed to be 0.3%, pH 6.9, 0.52 g/mL, 100-300 mm and 250 m²/g [134]. Removal of lead(II) ions was fitted well with the Langmuir isotherm due to the highest correlation efficiency (r^2 = 0.997) with the maximum adsorption capacity of 37.3 mg/g.

Pineapple based activated carbon: Several types of parts such as leaf, stem, crown, peel and pine apple wastes were used to prepare activated carbon under carbonization and activation process. The zinc chloride was used and the pyrolysis process was carried out at 500 °C for 60 min [135]. The activated carbon showed the highest surface area (914.67 m²/g) when the impregnation ratio was 1:1. The adsorption data supported Langmuir model (R^2 = 0.969) and showed maximum uptake of methylene blue about 288.34 mg/mL. The obtained carbon consisted of more oxygen containing functional group, micropores and mesoporous porosities when the starting material was pine apple crown leaf (activating agent was KOH) *via* microwave heating [136]. The adsorption capacity of methyl violet dye, which fitted well with the Redlich-Peterson model. Moreover, Noor & Nagendran [137] employed pine apple crown as raw material (under different activating agents). Percentage adsorption of methylene blue and malachite green dyes was observed to be 99.48% and 98.94% in H₃PO₄ treated carbon and 98.8% and 98.17%, respectively in NaOH treated carbon. Chan *et al.* [138] explained that the obtained pine apple stem based activated carbon showed the higher affinity on cationic (basic blue 3) as compared to anionic (Congo red) dye. Removal of basic blue 3 and Congo red dyes matched with Freundlich, Langmuir and Temin models because of the highest correlation coefficiency value, where R^2 = 0.998, 0.999 and 0.996, respectively. Moreover, the experimental results exhibited the best adsorption capacities for basic Blue 3 and Congo red dyes were observed to be 58.98 and 11.966 mg/g, respectively. The adsorption kinetic data supported pseudo-second order model and exothermic process [139]. Similarly, Weng *et al.* [140] reported that Freundlich model could be used to represent safranin-O cationic dye adsorption process (R^2 = 0.985), if compared to Langmuir model (R^2 = 0.9593). The highest adsorption capacities were 21.7 mg/g in the acidic conditions. The adsorption data fitted well with pseudo-second order model and Langmuir model. Rate of adsorption was increased with reducing the dye concentration (methylene blue) and ionic strength. The adsorption was spontaneous, exothermic, favourable at higher pH and lower temperature. The obtained results showed the highest adsorption capacities of methylene blue dye onto pine apple leaf powder based activated carbon could be observed (4.68×10^{-4} to 9.28×10^{-4} mol/g) with increasing the pH value (from 3.5 to 9.5). On the other hand, Rahmat *et al.* [141] reported the Langmuir model (R^2 = 0.9945) represented the removal of remazol brilliant blue R dye onto the pine apple leaf powder based activated carbon and the maximum mono-layer adsorption capacity reached 9.58 mg/g. The best adsorption capacity of crystal violet on to leaf powder carbon was observed to be 158.7 mg/g in specific conditions (pH = 8, particle size less than 150 μm, adsorbent dosage = 50 mg, temperature = 30 °C, agitation speed = 200 rpm) as reported by Shuvee *et al.* [142].

Banana based activated carbon: Activated carbon was produced in different conditions such as open air, nitrogen and steam conditions. It is observed that the surface area and percentage of yield can be tailored by controlling the activation conditions [143]. The highest surface area (204.23 m²/g) and yield (44.88%) could be observed in open air condition because of high ash content. The minimum yield (25.3%) and surface area (106.09 m²/g) could be seen in nitrogen gas and water steam conditions. The removal of arsenic(III) ions was spontaneous process, followed Langmuir model (Q_m = 142.86 mg/g) and pseudo-second order isotherm (Q_e = 18.52 mg/g, rate constant = 0.0111 g/(mg min). The banana peel was employed as starting material and showed several minerals (calcium = 56.4 mg/g), iron = 0.92 mg/g, manganese = 69.05 mg/g, niobium = 0.02 mg/g, potassium = 87.35 mg/g, rubidium = 2.51 mg/g, sodium = 22.5 mg/g, strontium = 0.02 mg and zirconium = 0.03 mg/g) [144]. The experiment results showed the faster removal of both dyes during the first 1 h (due to higher driving force from activated carbon), then increased slowly until 120 min for methylene blue (q_t = 105 mg/g) and 100 min for malachite green (q_t = 100 mg/g). Finally, reached equilibrium at 140 min for both studied dyes. Mondal & Kar *et al.* [145] explained the adsorption process was exothermic, spontaneous and adsorption capacity of Congo red dye reached 1.727 mg/g. The adsorption data supported Langmuir model and pseudo-second order kinetic isotherm.

Watermelon based activated carbon: Watermelon based activated carbon was produce to adsorb lead, iron copper, zinc, methylene blue, crystal violet, remazol brilliant blue reactive and rhodamine B dyes. The influence of carbonization temperature (200 to 350 ºC) on the ash (18.6-28.6%), volatile content (34-20.4%), fixed carbon (47.4-50.8) and yield (50-33%) was highlighted. The activated carbon treated with H_2SO_4 showed the best results if compared to zinc chloride and HCl. The results indicated 100% of lead(II), 90.6% of iron(III) and 99.1% of copper(II) were successfully removed by using 1 M H_2SO_4 [146]. The SEM analysis revealed watermelon rind has porous surface and consisted of inorganic and organic components. The highest removal of zinc(II), iron(III) and lead(II) ions was found to be 80%, 77% and 67%, respectively in actual domestic wastewater [147]. Lakshmipathy & Sarada [148] reported the loading capacity for methylene blue (489.8 mg/g), crystal violet (104.76 mg/g) and rhodamine B (86.6 mg/g) dyes. Thermodynamic studies revealed that the adsorption was exothermic, reduced in the randomness of solid-liquid interface, spontaneous for methylene blue and crystal violet dyes. The adsorption of remazol brilliant blue reactive dye onto activated carbon (surface area = 776.65 m^2/g, pore volume = 0.438 cm^3/g), fitted well with Freundlich model and pseudo-second order model [149]. The adsorption process was found to be spontaneous, endothermic and obeyed physical adsorption process (Dubinin-Radushkevich model).

Pomelo based activated carbon: Pomelo based activated carbon was prepared by using carbonization and KOH activation process, showed microporous, higher BET surface area (2504 m^2/g) and higher total pore volume (1.185 cm^3/g) [150]. The adsorption followed Langmuir model with the maximum adsorption of acid red 88 was 1486 mg/g. When the pomelo skin was used as precursor, the adsorption data showed Langmuir model, indicating monolayer adsorption for acid blue (444.45 mg/g) and methylene blue (501.1 mg/g) dyes onto the NaOH treated carbon [151]. Zheng *et al.* [152] reported that improvement of surface area (1.3 to 4.0845 m^2/g) through hydrothermal treatment. The adsorption capacity of Congo red dye was found to be 85 mg/g and 64 mg/g at 303 K and 323 K respectively, indicating the restrain hydrogen bonding between the functional groups within the dye compound. In acidic conditions, higher removal of dyes could be observed due to the dye compounds can attach with carboxyl groups of the activated carbon. The highest adsorption capacity was 144.93 mg/g, fitted well with Langmuir model and exothermic process. The prepared activated carbon (size = 75-180 μm) through carbonization (stove, nitrogen, 120 min, 550 ºC) and activation (K_2CO_3) process [153]. Surface area, micropore volume and total volume were 1213 m^2/g, 0.42 and 0.57, respectively. The results confirmed that when the activation time was increased, more new pores will be created, resulted in increased pore volume and surface area. However, at longer activation time, some produced pores could be destroyed. It was observed that the low impregnation ratio, resulted in inadequate contact between the activated carbon and activating agent. However, when the impregnation ratio was increased, enlarging pore volume and pore size because of sufficient contact was successfully improved. The adsorption kinetic

data supported pseudo-second order model (R^2 = 0.9985) if compared to other models, indicating the chemisorption process. The highest adsorption capacities of copper ions were 151.35 mg/g based on the Langmuir model (R^2 = 0.99). The effect of pH revealed that removal of copper(II) ion increased from 34.11 mg/g (pH 2) to 139.08 mg/g (pH 5). However, adsorption reduced when the pH beyond 5, indicating precipitation of metal hydroxide, resulted interfere with the adsorption process.

Grape based activated carbon: Several parts of grape such as seed, stalk and leave could be used to prepare activated carbon. The grape seed based activated carbon was produced *via* various activation agents. Under the specific conditions (100 mg/L adsorbate and 0.1 g activated carbon), the adsorption of nylosan red was 98%, 90.5% and 88.3% for KOH, H_3PO_4 and $CaCl_2$, respectively [154]. Davarnejad *et al.* [155] used grape stalk based activated carbon for the adsorption of methylene blue dye adsorption. The correlation coefficient (R^2) values was also reported *e.g.* Langmuir (R^2 = 0.99), Freundlich (R^2 = 0.615), Temkin (R^2 = 0.974) and Dubinin-Radushkevitch model (R^2 = 0.66). It was observed that the adsorption process was mono-layer and homogeneous, with the highest adsorption capacity (5.084 mg/g). On the other hand, Mousavi *et al.* [156] reported the grape leave based activated carbon was prepared in electric furnace, 120 min, 500 ºC under nitrogen atmosphere. The methylene blue dye removal percentage increased when the pH was increased from pH 3 to pH 11, indicating reduce in the electrostatic repulsion force between methylene blue and activated carbon. Higher correlation coefficient could be found in the Langmuir model (R^2 = 0.8894) with the highest adsorption capacity (0.2 mg/L) as compared to Freundlich model (R^2 = 0.58). Similarly, removal of heavy metal ions has also been reported by several researchers. Chand *et al.* [157] reported that the highest adsorption capacity of chromium(VI) ions was 1.91 mol/kg at pH 4 and followed the Langmuir model. Miralles *et al.* [158] also reported that Langmuir maximum removal of cadmium(II), lead(II), nickel(II) and copper(II) was 0.248, 0.241, 0.181 and 0.159 mmol/g, respectively.

Lemon based activated carbon: The precursors soaked in phosphoric acid, then carbonized in muffle furnace for 60 min, 500 ºC under nitrogen atmosphere as suggested by Sayed *et al.* [159]. Higher surface area (1158 m^2/g), higher percentage of yield (52.1%) and small amount of total ash (1.49%) was obtained. The highest correlation coefficient was observed in pseudo-second order model indicated the chemisorption process. Moreover, the intraparticle rate constant for malachite green dye and lead(II) ions was found to be 0.427 and 0.116 mg g^{-1} min$^{-1/2}$. When H_2SO_4 was used [160], an increased in the adsorption capacity of acid red 88 dye (16.91 to 25 mg/g) was observed when the adsorbent dose was increased (0.05 g to 0.25g). Based on the experimental results, the best conditions were temperature = 303 K, time = 40 min, pH = 2 and the dye concentration = 100 mg/L. Tejada-Tovar *et al.* [161] also reported the highest removal (62.1337%) of nickel(II) ion by using 0.355 mm (adsorbent size) as compared to other sizes. Based on response surface methodology (RSM), the best adsorption conditions could be found when adsorbent dose was 0.0783 g at 44.99 ºC. The thermodynamic parameters confirmed the

adsorption process was exothermic and non-spontaneous. Using lemon based activated carbon. Bukhari *et al.* [162] reported the monolayer adsorption capacity of eosin (anionic dye) 8.24 mg/g based on the Langmuir model. The adsorption was exothermic process and the kinetic data supported the chemisorption process.

Pomegranate based activated carbon: The pomegranate peel was dried, cleaned and crushed (150-300 µm) during the preparation process. Removal of copper(II), nickel(II), zinc(II) and cadmium(II) ions was found to be 0.074, 0.068, 0.073 and 0.075 mmol/g, respectively under the specific conditions (pH = 4.5, amount of adsorbent = 0.5 g). Thermodynamic studies revealed the positive value of entropy (0.1138 kJ/mol K) and enthalpy (25.84 kJ/mol), but the negative value of free energy (-7.51 to -9.64 kJ/mol) for the removal of copper(II) ion. Desorption studies indicated 79.5% of copper ions can be recovered by using 0.1 N HCl solution for desorption process [163]. The adsorption of chromium(VI) ions was carried out in the H_2SO_4 treated activated carbon [164]. Based on Langmuir model, the highest adsorption capacity of chromium(VI) ion was 35.2 mg/g. The intraparticle diffusion rate constants increased (0.15, 0.269, 0.421 to 0.45 mg g^{-1} min$^{-1/2}$) with increasing the direct red 28 dye concentration, indicating the adsorption rate was monitoring by the diffusion of dye within the adsorbent [165].

Date stones based activated carbon: Tunisian date stone based activated carbon was prepared under chemical activation (phosphoric acid), *via* specific pyrolysis temperature (450 ℃) and time (120 min) [166]. The surface area, total pore volume, average pore diameter, pH$_{zpc}$, particle size and carbon content were found to be 826 m^2/g, 0.46 cm^3/g, 2.25 nm, pH = 3.34, 100-160 and 91.3%, respectively. As observed from the SEM results, acid treated activated carbon showed very clear porous morphology as compared to raw date stones. In acidic conditions, low adsorption values due to competition between Pb^{2+} ions and H$^+$ ions for the adsorption process. In this experiment, adsorption of lead(II) ions increased from pH 3 to pH 6, reached maximum, then drops (pH 6 to pH 8) because of the formation of hydroxyl complexes. Thermodynamic studies revealed positive value of entropy (22.13 kcal/mol) and enthalpy (1.95 kcal/mol), indicating increase in the randomness and the adsorption was endothermic process. Ouahiba & Ahmed [167] described the synthesis of activated carbon from different types of date stone, *e.g.* Meh Degla and Ghares by using phosphoric acid (activating agent), under 600 ℃ in air atmosphere. The Meh Degla date stone based activated carbon exhibited high total pore volume (0.52 cm^3/g), high surface area (1060 m^2/g) as compared to Ghares date stone based activated carbon (765 m^2/g, 0.36 cm^3/g). Based on the Dubinin-Radushkevich model, the adsorption was physisorption, indicating the attraction of adsorbate to adsorbent by dispersion forces.

Durian based activated carbon: Durian peel, shell and seed were used to produce activated carbon under different conditions. Good quality durian peel based activated carbon was produced through chemical activation (H_3PO_4) and physical activation process (using nitrogen to develop pore formation). Phurada [168] reported the maximum removal of chromium ions at pH 2 and 30 min. The highest correlation coefficient value ($R^2 = 0.999$ and $R^2 = 0.979$) were found in pseudo-second order kinetic and Langmuir models (maximum adsorption capacity was 10.67 mg/g), respectively. Erny *et al.* [169] reported a well developed uniform pores could be observed by using durian shell, under chemical activation (0.6 M H_2O_2) at 700 ℃ for 30 min. It could be observed that 99% of methylene blue dye was removed.

Olive stone based activated carbon: Activated carbon could be prepared by using different types of olive stones. The results showed adsorption was exothermic, spontaneous and obey Freundlich model ($R^2 = 98\%$). It was observed that the highest nitrogen, hydrogen and carbon could be detected in black olive stones [170]. However, when the green olive stone was precursor, carbon showed higher entropy value and higher adsorption capacity of methylene blue dye (769 mg/g) could be observed. Corral-Bobadilla *et al.* [171] applied KOH activated adsorbent at 715 ℃ for 120 min for the maximum elimination of iron(III) ions (< 99%) in the optimized conditions. When phosphoric acid was used under specific conditions (heated in electric furnace at 380 ℃ for 2.5 h) [172], the surface area, average pore diameter, micropore volume and mesopore volume were observed to be 1194 m^2/g, 20.72 Å, 0.552 cm^3/g and 0.009 cm^3/g, respectively. The adsorption data obeyed Redlich-Peterson model and the highest removal capacity in lead(II) ion (147.5 mg/g) as compared to cadmium(II) (57.098 mg/g) and copper(II) (17.665 mg/g). Because of the biggest ionic radius could be observed in lead (1.19Å), followed by cadmium (0.95Å) and copper (0.73 Å). Similarly, Souad *et al.* [173] also synthesized olive stone based activated carbon *via* physical process. In this, the adsorption process reached the maximum equilibrium at 30 ℃ and the adsorption parameters supported Langmuir model with the maximum adsorption capacity of rhodamine B (217 mg/g) and Congo red (167 mg/g) dyes. The kinetic data followed simple intraparticle diffusion model.

Conclusion

The activated carbon has been produced by using different precursors, *via* carbonization and activation processes. The obtained carbon showed excellent surface area, high porosity structure and could be used as adsorbent to remove heavy metal ions and both anionic as well as cationic dyes successfully in the specific experimental conditions. The results confirmed that the activating agent could improve the adsorption capacity, surface area, porosity and pore volume as well. In general, activated carbon, which can be made from a wide variety of sources, is more effective for removing metal ions/dyes when it is evenly spread across the surface of a suitable support material. In addition, the thermodynamic studies indicated that the adsorption process is exothermic and spontaneous.

CONFLICT OF INTEREST

The authors declare that there is no conflict of interests regarding the publication of this article.

REFERENCES

1. Y. Xia, W. Li, X. He, D. Liu, Y. Sun, J. Chang and J. Liu, *Water*, **14**, 2446 (2022);
   https://doi.org/10.3390/w14152446

2. S. Alam, M.S. Khan, W. Bibi, I. Zekker, J. Burlakovs, M.M. Ghangrekar, G.D. Bhowmick, A. Kallistova, N. Pimenov and M. Zahoor, *Water*, **13**, 1453 (2021);
   https://doi.org/10.3390/w13111453

3. A. Dabrowski, *Adv. Colloid Interface Sci.*, **93**, 135 (2001);
   https://doi.org/10.1016/S0001-8686(00)00082-8

4. H. Karge and J. Weitkamp, Adsorption and Diffusion, Springer: Berlinp, pp. 1-45 (2008).

5. R. Bansal and M. Goyal, Activated Carbon Adsorption. CRC Press, Florida, United States, pp. 1-66 (2005).

6. M. Sulyman, J. Namiesnik and A. Gierak, *Pol. J. Environ. Stud.*, **26**, 479 (2017);
   https://doi.org/10.15244/pjoes/66769

7. C. Mahamadi and T. Nharingo, *Bioresour. Technol.*, **101**, 859 (2010);
   https://doi.org/10.1016/j.biortech.2009.08.097

8. D. Sud, G. Mahajan and M. Kaur, *Bioresour. Technol.*, **99**, 6017 (2008);
   https://doi.org/10.1016/j.biortech.2007.11.064

9. F. Fu and Q. Wang, *J. Environ. Manage.*, **92**, 407 (2011);
   https://doi.org/10.1016/j.jenvman.2010.11.011

10. B. Volesky, *Hydrometallurgy*, **59**, 203 (2001);
    https://doi.org/10.1016/S0304-386X(00)00160-2

11. F. Hai, K. Yamamoto, F. Nakajima and K. Fukushi, *Water Res.*, **45**, 2199 (2011);
    https://doi.org/10.1016/j.watres.2011.01.013

12. M. Ormad, N. Miguel, A. Claver, M. Matesanz and J. Ovelleiro, *Chemosphere*, **71**, 97 (2008);
    https://doi.org/10.1016/j.chemosphere.2007.10.006

13. W. Hijnen, G. Suylen, J. Bahlman, A. Brouwer-Hanzens and G.J. Medema, *Water Res.*, **44**, 1224 (2010);
    https://doi.org/10.1016/j.watres.2009.10.011

14. M. Nahil and P. Williams, *J. Anal. Appl. Pyrolysis*, **91**, 67 (2011);
    https://doi.org/10.1016/j.jaap.2011.01.005

15. T. Khadiran, M. Hussein, Z. Zainal and R. Rusli, *BioResources*, **10**, 986 (2015).

16. M. Zaini and M. Kamaruddin, *J. Anal. Appl. Pyrolysis*, **101**, 238 (2013);
    https://doi.org/10.1016/j.jaap.2013.02.003

17. B. Zhang, Y. Liu and Y. Ye, *Mod. Chem. Ind.*, **34**, 34 (2014).

18. G. Oh and C. Park, *Fuel*, **81**, 327 (2002);
    https://doi.org/10.1016/S0016-2361(01)00171-5

19. I.D. Canan and S.H. Demiral, *Surf. Interf.*, **22**, 100873 (2021);
    https://doi.org/10.1016/j.surfin.2020.100873

20. A. Basta, V. Fierro, H. El-Saied and A. Celzard, *Bioresour. Technol.*, **100**, 3941 (2009);
    https://doi.org/10.1016/j.biortech.2009.02.028

21. M.K. Jha, S. Joshi, R.K. Sharma, A.A. Kim, B. Pant, M. Park and H.R. Pant, *Nanomaterials*, **11**, 3140 (2021);
    https://doi.org/10.3390/nano11113140

22. A. Houshmand, M.S. Shafeeyan, A. Arami-Niya and W.M.A.W. Daud, *J. Taiwan Inst. Chem. Eng.*, **44**, 774 (2013);
    https://doi.org/10.1016/j.jtice.2013.01.014

23. S. Mahanim, W. Asma, J. Rafidah, E. Puad and H. Shaharuddin, *J. Trop. Forest Sci.*, **23**, 417 (2011).

24. Activated Carbon Market; https://www.marketsandmarkets.com/Market-Reports/activated-carbon-362.html

25. F. Pua, M.S. Sajab, C.H. Chia, S. Zakaria, I.A. Rahman and M.S. Salit, *J. Environ. Chem. Eng.*, **1**, 460 (2013);
    https://doi.org/10.1016/j.jece.2013.06.012

26. F. Ahmad, W.M.A.W. Daud, M.A. Ahmad and R. Radzi, *Chem. Eng. Res. Des.*, **90**, 1480 (2012);
    https://doi.org/10.1016/j.cherd.2012.01.017

27. G. Cruz, M. Pirilä, R. Finland, M. Huuhtanen and L. Carrión, *J. Civil Environ. Eng.*, **2**, 109 (2012);
    https://doi.org/10.4172/2165-784X.1000109

28. M.C. Ribas, M.A. Adebayo, L.D.T. Prola, E.C. Lima, R. Cataluña, L.A. Feris, M.J. Puchana-Rosero, F.M. Machado, F.A. Pavan and T. Calvete, *Chem. Eng. J.*, **248**, 315 (2014);
    https://doi.org/10.1016/j.cej.2014.03.054

29. S. Mylsamy and C. Theivarasu, *World J. Appl. Environ. Chem.*, **1**, 22 (2012).

30. N. Meunier, J. Laroulandie, J.F. Blais and R.D. Tyagi, *Bioresour. Technol.*, **90**, 255 (2003);
    https://doi.org/10.1016/S0960-8524(03)00129-9

31. A.Y. León, J.R. Rincón, N. Rodríguez and D.R. Molina, *Int. J. Environ. Sci. Technol.*, **19**, 7777 (2022);
    https://doi.org/10.1007/s13762-021-03687-3

32. M.E. Fernandez, G.V. Nunell, P.R. Bonelli and A.L. Cukierman, *Ind. Crops Prod.*, **62**, 437 (2014);
    https://doi.org/10.1016/j.indcrop.2014.09.015

33. A. Khaled, A. El Nemr, A. El-Sikaily and O. Abdelwahab, *J. Hazard. Mater.*, **165**, 100 (2009);
    https://doi.org/10.1016/j.jhazmat.2008.09.122

34. M. Amaal and H. Ali, *J. Appl. Sci*, **3**, 13 (2017).

35. F. Lahieb, A. Shahad and T. Zainab, *J. Green Eng.*, **10**, 10600 (2020).

36. A. Osman, J. Blewitt, K. Abu-Dahrieh, C. Farrell, A.H. Al-Muhtaseb, J. Harrison and D.W. Rooney, *Environ. Sci. Pollut. Res. Int.*, **26**, 37228 (2019);
    https://doi.org/10.1007/s11356-019-06594-w

37. M. El-Azazy, A.S. El-Shafie, A.A. Issa, M. Al-Sulaiti, J. Al-Yafie, B. Shomar and K. Al-Saad, *J. Chem.*, **2019**, 4926240 (2019);
    https://doi.org/10.1155/2019/4926240

38. E.-K. Guechi and O. Hamdaoui, *Desalin. Water Treat.*, **57**, 10677 (2016);
    https://doi.org/10.1080/19443994.2015.1038739

39. E. Hoseinzadeh, M.-R. Samarghandi, G. McKay, N. Rahimi and J. Jafari, *Desalin. Water Treat.*, **52**, 4999 (2014);
    https://doi.org/10.1080/19443994.2013.810355

40. K. Ben Jeddou, F. Bouaziz, F. Ben Taheur, O. Nouri-Ellouz, R. Ellouz-Ghorbel and S. Ellouz-Chaabouni, *Water Sci. Technol.*, **83**, 1384 (2021);
    https://doi.org/10.2166/wst.2021.075

41. H. Saygili and F. Güzel, *J. Clean. Prod.*, **113**, 995 (2016);
    https://doi.org/10.1016/j.jclepro.2015.12.055

42. K. Fu, Q. Yue, B. Gao, Y. Wang and Q. Li, *Colloids Surf. A Physicochem. Eng. Asp.*, **529**, 842 (2017);
    https://doi.org/10.1016/j.colsurfa.2017.06.064

43. R. Mallampati and S. Valiyaveettil, *RSC Adv.*, **2**, 9914 (2012);
    https://doi.org/10.1039/c2ra21108d

44. R. Carlos, A. Pena, B. Duran and Y. Gozalez, Proceedings of ICERI2011 Conference, 14th -16th November 2011, Madrid, Spain, pp. 1552-1560 (2011).

45. M.A. Chimdessa and B.A. Ejeta, *Orient. J. Chem.*, **38**, 65 (2022);
    https://doi.org/10.13005/ojc/380107

46. M. Ait Haki, A. Imgharn, N. Aarab, A. Hsini, A. Essekri, M. Laabd, H. El Jazouli, M. Elamine, R. Lakhmiri and A. Albourine, *Water Sci. Technol.*, **85**, 433 (2022);
    https://doi.org/10.2166/wst.2021.451

47. C. Palma, L. Lloret, A. Puen, M. Tobar and E. Contreras, *Chin. J. Chem. Eng.*, **24**, 521 (2016);
    https://doi.org/10.1016/j.cjche.2015.11.029

48. N. Priyantha, L.B.L. Lim, M.K. Dahri and D.T.B. Tennakoon, *J. Appl. Sci. Environ. Sanit.*, **8**, 179 (2013).

49. A. Sahriani, N. La and P. Taba, *Indones. Chim. Acta*, **11**, 21 (2018);
    https://doi.org/10.20956/ica.v11i1.6401

50. M. Tanasal, N. La and P. Taba, *Indones. Chim. Acta*, **8**, 18 (2015);
    https://doi.org/10.20956/ica.v8i1.2478

51. N. Priyantha, L. Lim and M. Dahri, *Int. Food Res. J.*, **22**, 2141 (2015).

52. A.H. Jawad, A. Saud Abdulhameed, L.D. Wilson, S.S.A. Syed-Hassan, Z.A. ALOthman and M. Rizwan Khan, *Chin. J. Chem. Eng.*, **32**, 281 (2021);
    https://doi.org/10.1016/j.cjche.2020.09.070

53. O. Oribayo, O. Olaleye, A. Akinyanju, O. Omoloja and S.O. Williams, *Niger. J. Technol.*, **39**, 1076 (2021);
    https://doi.org/10.4314/njt.v39i4.14

54. S. Srisorrachatr, P. Kri-arb, S. Sukyang and C. Jumruen, *MATEC Web Conf.*, **119**, 01019 (2017);
    https://doi.org/10.1051/matecconf/201711901019

55. J. Bernard and O. Odigure, *Res. J. Chem. Sci.*, **3**, 3 (2013).

56. L. Onyeji and A. Aboje, *Int. J. Eng. Sci. Technol.*, **3**, 8238 (2011).

57. D.D.T.T.D. Senarathna, V. Thangarajah, K.H.D.N. Abeysooriya, W.M.Y.H. Wijesundara, A.H.M.L.N. Kumari and M.G.G.S.N. Thilakarathna, *Am. J. Anal. Chem.*, **11**, 389 (2020);
    https://doi.org/10.4236/ajac.2020.1112031

58. M. Basu, K. Guha and L. Ray, *J. Clean. Prod.*, **151**, 603 (2017);
https://doi.org/10.1016/j.jclepro.2017.03.028

59. M. Basu, A.K. Guha and L. Ray, *Indian Chem. Eng.*, **60**, 179 (2017);
https://doi.org/10.1080/00194506.2017.1341349

60. T. Smitha, T. Santhi, A.L. Prasad and S. Manonmani, *Arab. J. Chem.*, **10**, S244 (2017);
https://doi.org/10.1016/j.arabjc.2012.07.030

61. G. Vasu and S. Selvaraju, Adsorptive Removal of Copper by Cucumber Peel Adsorbent: Isotherm, Kinetics and Mass Transfer Studies, In: Sustainable Bio-nano Materials and Macromolecules for Textile Wastewater Treatment, Publisher, Springer, pp. 1-30 (2022).

62. C.T. Weber, E.L. Foletto and L. Meili, *Water Air Soil Pollut.*, **224**, 1427 (2013);
https://doi.org/10.1007/s11270-012-1427-7

63. M. Ahmaruzzaman, *Sep. Sci. Technol.*, **47**, 2381 (2012);
https://doi.org/10.1080/01496395.2012.671432

64. W. Igwegbe, B. Okoro and J. Osuagwu, *Int. J. Environ. Chem. Ecol. Geol. Geophys. Eng.*, **9**, 1400 (2015).

65. A. Saeed, M. Akhter and M. Iqbal, *Sep. Purif. Technol.*, **45**, 25 (2005);
https://doi.org/10.1016/j.seppur.2005.02.004

66. U. Ladhe and R. Patil, *Int. J. Sci. Environ. Technol.*, **3**, 546 (2014).

67. M. Zayat and E. Smith, *Can. J. Environ. Constr. Civ. Eng.*, **1**, 71 (2010).

68. L. Zhang, J. Tan, G. Xing, X. Dou and X. Guo, *Bioresour. Bioprocess.*, **8**, 10 (2021);
https://doi.org/10.1186/s40643-021-00364-8

69. N. Djordjevic, M. Miljkovic and S. Urosevic, *Izv. Him.*, **46**, 277 (2014).

70. K. Mohanty, J.T. Naidu, B.C. Meikap and M.N. Biswas, *Ind. Eng. Chem. Res.*, **45**, 5165 (2006);
https://doi.org/10.1021/ie060257r

71. M. Ahiduzzaman and A.K.M. Sadrul Islam, *Springerplus*, **5**, 1248 (2016);
https://doi.org/10.1186/s40064-016-2932-8

72. M. Emadi and M.A. Zare, *J. Water Res. Eng.*, **4**, 98 (2012).

73. F. Hanum, O. Bani and L.I. Wirani, *IOP Conf. Ser. Mater. Sci. Eng.*, **180**, 012151 (2017);
https://doi.org/10.1088/1757-899X/180/1/012151

74. N.T. Abdel-Ghani, G.A. El-Chaghaby and E.M. Zahran, *Am. J. Anal. Chem.*, **6**, 71 (2015);
https://doi.org/10.4236/ajac.2015.61007

75. N. Abbas, H. Zahraa and H. Ahmed, *Iraqi Nat. J. Chem.*, **51**, 273 (2013).

76. M. Imamoglu and O. Tekir, *Desalination*, **228**, 108 (2008);
https://doi.org/10.1016/j.desal.2007.08.011

77. O.T. Dede, *J. Eng. Sci. Des.*, **7**, 301 (2019);
https://doi.org/10.21923/jesd.486065

78. B. Veselin, M. Novakovic, A. Dragan and M. Dusan, 28th International Conference Ecological Truth & Environmental Research, 16-19 June 2020, Kladovo, Serbia (2020).

79. N. Walaikorn, W. Yada, J. Thanut and E. Kamontip, *Chiang Mai J. Sci.*, **42**, 407 (2015).

80. T. Nakamura, T. Tokimoto, T. Tamura, N. Kawasaki and S. Tanada, *J. Health Sci.*, **49**, 520 (2003);
https://doi.org/10.1248/jhs.49.520

81. I. Block, C. Günter, A. Duarte Rodrigues, S. Paasch, P. Hesemann and A. Taubert, *Materials*, **14**, 3996 (2021);
https://doi.org/10.3390/ma14143996

82. G. Kyzas, *Materials*, **5**, 1826 (2012);
https://doi.org/10.3390/ma5101826

83. L. Giraldo and J.C. Moreno-Piraján, *E-J. Chem.*, **9**, 938 (2012);
https://doi.org/10.1155/2012/120763

84. G. Sreelatha and P. Padmaja, *J. Environ. Prot. Sci.*, **2**, 63 (2008).

85. J.R. García, U. Sedran, M.A.A. Zaini and Z.A. Zakaria, *Environ. Sci. Pollut. Res. Int.*, **25**, 5076 (2018);
https://doi.org/10.1007/s11356-017-8975-8

86. W.T. Mook, M.K. Aroua and M. Szlachta, *BioResources*, **11**, 1432 (2016);
https://doi.org/10.15376/biores.11.1.1432-1447

87. R. Baby, B. Saifullah and M.Z. Hussein, *Sci. Rep.*, **9**, 18955 (2019);
https://doi.org/10.1038/s41598-019-55099-6

88. M. Imran-Shaukat, R. Wahi, N.R. Rosli, S.M.A. Aziz and Z. Ngaini, *IOP Conf. Ser. Earth Environ. Sci.*, **765**, 012019 (2021);
https://doi.org/10.1088/1755-1315/765/1/012019

89. S.E.M. Saber, S.B.A. Rahim, H. Wan Yussof, O.A. Olalere and O.A. Habeeb, *Chem. Data Collect.*, **21**, 100235 (2019);
https://doi.org/10.1016/j.cdc.2019.100235

90. Z. Li, H. Hanafy, L. Zhang, L. Sellaoui, M.S. Netto, M.L.S. Oliveira, M.K. Seliem, G. Luiz Dotto, A. Bonilla-Petriciolet and Q. Li, *Chem. Eng. J.*, (2020);
https://doi.org/10.1016/j.cej.2020.124263

91. M. Uddin and A. Nasar, *Sci. Rep.*, **10**, 7983 (2020);
https://doi.org/10.1038/s41598-020-64745-3

92. M. Ashrafi, G. Bagherian, M.A. Chamjangali and N. Goudarzi, *Anal. Bioanal. Chem. Res.*, **5**, 95 (2018).

93. M.K. Dahri, M.R.R. Kooh and L.B.L. Lim, *J. Mater. Environ. Sci.*, **8**, 3706 (2017).

94. P. Maheswari, N. Venilamani, S. Madhavakrishnan, P.S.S. Shabudeen, R. Venckatesh and S. Pattabhi, *E-J. Chem.*, **5**, 233 (2008);
https://doi.org/10.1155/2008/376839

95. M. Karthika and M.Vasuki, *Mater. Today Proc.*, **14**, 358 (2019);
https://doi.org/10.1016/j.matpr.2019.04.158

96. N. Zainab, R. Wahi, H. Hussain and Q. Nurul, In: THE 3rd International Conference On Separation Technology 2020 -VIRTUAL (ICoST 2020), 15 August 2020 (2021),
https://doi.org/10.1007/978-981-16-0742-4_14

97. H. Hameed and M. Daud, *Chem. Eng. J.*, **139**, 48 (2008);
https://doi.org/10.1016/j.cej.2007.07.089

98. L. Linh, E. Usama, N. Mansor and Y. Uemura, *Int. J. Biomass Renew.*, **1**, 32 (2012).

99. H. Zakaria, M.A.K.M. Hanafiah, W.S.W. Ngah, S.C. Ibrahim and W.A.H.W. Ilias, *J. Appl. Sci.*, **6**, 2762 (2006);
https://doi.org/10.3923/jas.2006.2762.2767

100. A. Ahmad and R. Alrozi, *Chem. Eng. J.*, **171**, 510 (2011);
https://doi.org/10.1016/j.cej.2011.04.018.

101. M.A. Ahmad, N.S. Afandi, K.A. Adegoke and O.S. Bello, *Desalination Water Treat.*, **57**, 21487 (2016);
https://doi.org/10.1080/19443994.2015.1119744

102. M.A. Ahmad and R. Alrozi, *Chem. Eng. J.*, **168**, 280 (2011);
https://doi.org/10.1016/j.cej.2011.01.005

103. K.S. Tarigan, B. Haryanto, R. Tambun, K. Manik and A.K. Lumbangaol, *J. Phys. Conf. Ser.*, **1542**, 012047 (2019);
https://doi.org/10.1088/1742-6596/1542/1/012047

104. R. Rinaldi, Y. Yasdi and W.L.C. Hutagalung, *AIP Conf. Proc.*, **2026**, 020098 (2018);
https://doi.org/10.1063/1.5065058

105. C. Bijang, M.F.J.D.P. Tanasale, D. Sri, T. Tahril and T. Azis, *J. Akad. Kim.*, **11**, 56 (2022);
https://doi.org/10.22487/j24775185.2022.v11.i1.pp56-63

106. M.K. Dahri, L.B.L. Lim and C.C. Mei, *Environ. Monit. Assess.*, **187**, 546 (2015);
https://doi.org/10.1007/s10661-015-4768-z

107. D. Khairud, L. Lim, P. Namal and M. Chan, *Int. Food Res. J.*, **23**, 1154 (2016).

108. R. Duraisamy, M. Mechoro, T. Seda and M. Akhtar Khan, *Cogent Eng.*, **7**, 1813237 (2020);
https://doi.org/10.1080/23311916.2020.1813237

109. K.A. Adegoke, O. Adeleke, M.O. Adesina, R.O. Adegoke and O.S. Bello, *Curr. Res Green Sustain. Chem.*, **5**, 100275 (2022);
https://doi.org/10.1016/j.crgsc.2022.100275

110. C. Bose, P. Banerjee, J. Kundu, B. Dutta, I. Ghosh, S. Sinha, A. Ghosh, A. Barua, S. Gupta, U. Das, S.S. Jana and S. Sinha, *ChemistrySelect*, **5**, 14168 (2020);
https://doi.org/10.1002/slct.202003322

111. C. Phawachalotorn and N. Suwanpayak, *J. Phys. Conf. Ser.*, **1719**, 012061 (2021);
https://doi.org/10.1088/1742-6596/1719/1/012061

112. M.A. Ahmad and R. Alrozi, *Chem. Eng.*, **165**, 883 (2010);
https://doi.org/10.1016/j.cej.2010.10.049

113. Y. Chen, M. Huang, W. Chen and B. Huang, *BioResources*, **7**, 4965 (2012).

114. A. El-Saharty, S.N. Mahmoud, A.H. Manjood, A.A.H. Nassar and A.M. Ahmed, *Int. J. Ecotoxicol. Ecobiol.*, **3**, 51 (2018);
https://doi.org/10.11648/j.ijee.20180302.13

115. M. Abbas, *Mater. Today Proc.*, **43**, 3359 (2021);
https://doi.org/10.1016/j.matpr.2020.05.320

116. M. Kerrou, N. Bouslamti, A. Raada, A. Elanssari, D. Mrani and M.S. Slimani, *Int. J. Anal. Chem.*, **2021**, 5570806 (2021);
https://doi.org/10.1155/2021/5570806

117. M.A.M. Razi, A.A. Gheethi and I.A. Za, *Int. J. Eng. Technol.*, **7**, 112 (2018); https://doi.org/10.14419/ijet.v7i4.30.22066

118. B.A. Ezeonuegbu, D.A. Machido, C.M.Z. Whong, W.S. Japhet, A. Alexiou, S.T. Elazab, N. Qusty, C.A. Yaro and G.E.-S. Batiha, *Biotechnol. Rep.*, **30**, e00614 (2021); https://doi.org/10.1016/j.btre.2021.e00614

119. G.M. Santana, R.C.C. Lelis, J.B. Paes, R.M. Morais, C.R. Lopes and C.R. Lima, *Cienc. Florest.*, **28**, 1179 (2018); https://doi.org/10.5902/1980509833395

120. Y.-J. Zhang, J.-L. Ou, Z.-K. Duan, Z.-J. Xing and Y. Wang, *Colloids Surf. A Physicochem. Eng. Asp.*, **481**, 108 (2015); https://doi.org/10.1016/j.colsurfa.2015.04.050

121. S. Chan, W. Cheung and G. McKay, *Desalination*, **218**, 304 (2008); https://doi.org/10.1016/j.desal.2007.02.026

122. F. Ademiluyi and A. Ujile, *Int. J. Eng. Technol.*, **3**, 623 (2013).

123. K. Masood, A. Amanual, D. Ramesh and B. Kerebo, *Int. J. Water Res.*, **5**, 33 (2015).

124. G. McConnachie, A. Warhurst, S. Pollard and V. Chipofya, In: 22nd WEDC Conference, New Delhi, India, pp. 279-282 (1996).

125. T.H. Do, V.T. Nguyen, N.Q. Dung, M.N. Chu, D. Van Kiet, T.T.K. Ngan and L. Van Tan, *Mater. Today Proc.*, **38**, 3405 (2021); https://doi.org/10.1016/j.matpr.2020.10.834

126. I.M. Reck, R.M. Paixão, R. Bergamasco, M.F. Vieira and A.M.S. Vieira, *J. Clean. Prod.*, **171**, 85 (2018); https://doi.org/10.1016/j.jclepro.2017.09.237

127. M. Matouq, N. Jildeh, M. Qtaishat, M. Hindiyeh and M.Q. Al Syouf, *J. Environ. Chem. Eng.*, **3**, 775 (2015); https://doi.org/10.1016/j.jece.2015.03.027

128. M.S. Azad, M.S. Hassan, S. Azhari and M. Shahinuzzaman, *Int. J. Eng. Res. Technol. (Ahmedabad)*, **9**, 695 (2020).

129. N. Zawani, N. Aina, A. Siti and M. Lias, *J. Int. UiTM Perlis*, **7**, 22 (2012).

130. E. Sayed, H. Aly and H. Hussien, *Int. J. Res. Chem. Environ.*, **1**, 132 (2011).

131. G.O. El-Sayed, M.M. Yehia and A.A. Asaad, *Water Resour. Ind.*, **7-8**, 66 (2014); https://doi.org/10.1016/j.wri.2014.10.001

132. H.-J. Choi and S.-W. Yu, *Environ. Eng. Res.*, **24**, 99 (2019); https://doi.org/10.4491/eer.2018.107

133. S. Preethi, A. Sivasamy, S. Sivanesan, V. Ramamurthi and G. Swaminathan, *Ind. Eng. Chem. Res.*, **45**, 7627 (2006); https://doi.org/10.1021/ie0604122

134. S. Hashemian, K. Salari, H. Salehifar and Z.A. Yazdi, *E-J. Chem.*, **2013**, 283274 (2013); https://doi.org/10.1155/2013/283274

135. M.N. Mahamad, M.A.A. Zaini and Z.A. Zakaria, *Int. Biodeter. Biodegr.*, **102**, 274 (2015); https://doi.org/10.1016/j.ibiod.2015.03.009

136. W. Astuti, T. Sulistyaningsih, E. Kusumastuti, G.Y.R.S. Thomas and R.Y. Kusnadi, *Bioresour. Technol.*, 287, 121426 (2019); https://doi.org/10.1016/j.biortech.2019.121426

137. S. Nagendran and S. Noor, *APRN Eng. Appl. Sci.*, **10**, 9476 (2015).

138. S.-L. Chan, Y.P. Tan, A.H. Abdullah and S.-T. Ong, *J. Taiwan Inst. Chem. Eng.*, **61**, 306 (2016); https://doi.org/10.1016/j.jtice.2016.01.010

139. A. Shitu, M. Mohammed and A. Ibrahim, *Int. J. Environ. Monit. Anal.*, **2**, 128 (2014); https://doi.org/10.11648/j.ijema.20140203.11

140. C. Weng, Y. Lin and T. Tzeng, *J. Hazard. Mater.*, **170**, 417 (2009); https://doi.org/10.1016/j.jhazmat.2009.04.080

141. N.A. Rahmat, A.A. Ali, Salmiati, N. Hussain, M.S. Muhamad, R.A. Kristanti and T. Hadibarata, *Water Air Soil Pollut.*, **227**, 105 (2016); https://doi.org/10.1007/s11270-016-2807-1

142. S. Neupane, S.T. Ramesh, R. Gandhimathi and P.V. Nidheesh, *Desalin. Water Treat.*, **54**, 2041 (2015); https://doi.org/10.1080/19443994.2014.903867

143. V.K. Jha and J. Maharjan, *Sci. World*, **15**, 145 (2022); https://doi.org/10.3126/sw.v15i15.45665

144. M. Dahiru, Z.U. Zango and M.A. Haruna, *Am. J. Mater. Sci.*, **8**, 32 (2018); https://doi.org/10.5923/j.materials.20180802.02

145. N.K. Mondal and S. Kar, *Appl. Water Sci.*, **8**, 157 (2018); https://doi.org/10.1007/s13201-018-0811-x

146. W. Gin, A. Jimoh, A. Giwa and A. Abdulkareem, *Int. J. Sci. Eng. Res.*, **5**, 66 (2014).

147. N. Othman, N. Azhar, P.S.M.A. Rani and H.M. Zaini, *MATEC Web Conf.*, (2016); https://doi.org/10.1051/matecconf/20167801028

148. R. Lakshmipathy and N. Sarada, *Desalin. Water Treat.*, **52**, 6175 (2014); https://doi.org/10.1080/19443994.2013.812526

149. M.A. Ahmad, N. Ahmad and O.S. Bello, *J. Dispers. Sci. Technol.*, **36**, 845 (2015); https://doi.org/10.1080/01932691.2014.925400

150. Z. Liu and K. Xing, *J. Chem.*, **2021**, 6617934 (2021); https://doi.org/10.1155/2021/6617934

151. Y. Foo and H. Hameed, *Chem. Eng. J.*, **173**, 385 (2011); https://doi.org/10.1016/j.cej.2011.07.073

152. H. Zheng, Q. Sun, Y. Li and Q. Du, *Mater. Res. Express*, **7**, 045505 (2020); https://doi.org/10.1088/2053-1591/ab8a83

153. Z. Liu and Y. Wei, *J. Chem.*, **2021**, 9940577 (2021); https://doi.org/10.1155/2021/9940577

154. M. Hamzaoui, B. Bestani, N. Benderdouche, O. Douinat and Z. Mekkibe, *Int. J. Sci. Res. Chem. Sci.*, **7**, 11 (2020).

155. R. Davarnejad, S. Afshar and P. Etehadfar, *Arab. J. Chem.*, **13**, 5463 (2020); https://doi.org/10.1016/j.arabjc.2020.03.025

156. S.A. Mousavi, A. Mahmoudi, S. Amiri, P. Darvishi and E. Noori, *Appl. Water Sci.*, **12**, 112 (2022); https://doi.org/10.1007/s13201-022-01648-w

157. R. Chand, K. Narimura, H. Kawakita, K. Ohto, T. Watari and K. Inoue, *J. Hazard. Mater.*, **163**, 245 (2009); https://doi.org/10.1016/j.jhazmat.2008.06.084

158. N. Miralles, M. Martínez, A. Florido, I. Casas, N. Fiol and I. Villaescusa, *Solvent Extr. Ion Exch.*, **26**, 261 (2008); https://doi.org/10.1080/07366290802053660

159. S.Z. Mohammadi, M.A. Karimi, S.N. Yazdy, T. Shamspur and H. Hamidian, *Quim. Nova*, **37**, 804 (2014); https://doi.org/10.5935/0100-4042.20140129

160. M. Azam, M.B. Lohani, A.R. Khan, Q.I. Rahman and G.R. Lohani, *TEST Eng. Manage.*, **82**, 4138 (2020).

161. C. Tejada-Tovar, A. Villabona-Ortíz, C. Sierra-Ardila, M. Meza-Acuña and R. Ortega-Toro, *Rev. Fac. Ing. Univ. Antioquia*, **101**, 31 (2021); https://doi.org/10.17533/udea.redin.20200691

162. A. Bukhari, I. Ijaz, H. Zain, E. Gilani, A. Nazir, A. Bukhari, S. Raza, J. ansari, S. Hussain, S.S. Alarfaji, R. saeed, Y. Naseer, R. Aftab and S. Iram, *Arab. J. Chem.*, **15**, 103873 (2022); https://doi.org/10.1016/j.arabjc.2022.103873

163. R.A.K. Rao and F. Rehman, *Adsorpt. Sci. Technol.*, **28**, 195 (2010); https://doi.org/10.1260/0263-6174.28.3.195

164. A. Nemr, *J. Hazard. Mater.*, **161**, 132 (2009); https://doi.org/10.1016/j.jhazmat.2008.03.093

165. R. Venckatesh, T. Amuha, R. Sivaraj and M. Chandramohan, *Int. J. Eng. Sci. Technol.*, **2**, 2040 (2010).

166. F. Bouhamed, Z. Elouear, J. Bouzid and B. Ouddane, *Desalin. Water Treat.*, **52**, 2261 (2014); https://doi.org/10.1080/19443994.2013.806222

167. B. Ouahiba and A. Ahmed, *Der Pharma Chem.*, **8**, 344 (2016).

168. S. Phurada, In 2011 International Conference on Biotechnology and Environment Management, pp. 33-38 (2011).

169. H. Erny, S. Melissa, S. Suriati and Z. Ku, *Key Eng. Mater.*, **594-595**, 350 (2014).

170. M.A. Al-Ghouti and A.O. Sweleh, *Environ. Technol. Innov.*, **16**, 100488 (2019); https://doi.org/10.1016/j.eti.2019.100488

171. M. Corral-Bobadilla, R. Lostado-Lorza, F. Somovilla-Gómez and R. Escribano-García, *J. Clean. Prod.*, **294**, 126332 (2021); https://doi.org/10.1016/j.jclepro.2021.126332

172. T. Bohli, A. Ouederni, N. Fiol and I. Villaescusa, *C.R. Chim.*, **18**, 88 (2015); https://doi.org/10.1016/j.crci.2014.05.009

173. S. Najar-Souissi, A. Ouederni and A. Ratel, *J. Environ. Sci. (China)*, **17**, 998 (2005).